

SUPPORTING INFORMATION

Non-Symmetric Cysteine Stapling in Native Peptides and Proteins

Sven Ullrich,^{a,b,‡,*} Bishvanwasha Panda,^{a,‡} Upamali Somathilake,^a Douglas J. Lawes,^a and
Christoph Nitsche^{a,*}

^a Research School of Chemistry, Australian National University, Canberra 2601 ACT, Australia

^b Present address: Department of Chemistry, Graduate School of Science, University of Tokyo, Bunkyo-ku, Tokyo 113-0033, Japan

[‡] These authors contributed equally: Sven Ullrich, Bishvanwasha Panda.

^{*} Correspondence to: sullrich@g.ecc.u-tokyo.ac.jp; christoph.nitsche@anu.edu.au.

Contents

Abbreviations.....	S3
Materials	S5
Linear peptide synthesis.....	S5
HPLC purification.....	S7
LCMS analysis.....	S9
Peptide stapling.....	S15
Buffer and concentration variations.....	S15
Stapling kinetics.....	S15
Azide-alkyne cycloaddition	S28
HRMS analysis	S29
SPR analysis	S36
Protease inhibition assay.....	S38
Protease stability assay	S41
Protein expression.....	S43
Protein purification	S44
Protein mass spectrometry	S45
Protein stapling	S45
Molecule visualisation	S45
NMR spectroscopy.....	S50
Supporting references	S51

Abbreviations

AMC	7-amino-4-methylcoumarin
BTAA	2-(4-((bis((1-(<i>tert</i> -butyl)-1 <i>H</i> -1,2,3-triazol-4-yl)methyl)amino)methyl)-1 <i>H</i> -1,2,3-triazol-1-yl)acetic acid
DIPEA	<i>N,N</i> -diisopropylethylamine
DMA	<i>N,N</i> -dimethylacetamide
DMF	<i>N,N</i> -dimethylformamide
EDC	1-ethyl-3-(3-dimethylaminopropyl)carbodiimide
EDT	1,2-ethanedithiol
EDTA	ethylenediaminetetraacetic acid
ESI	electrospray ionisation
Fmoc-AA	<i>N</i> _α -fluorenylmethoxycarbonyl protected amino acid
FPLC	fast protein liquid chromatography
GFP	green fluorescent protein
HBTU	hexafluorophosphate benzotriazole tetramethyl uranium
HEPES	4-(2-hydroxyethyl)-1-piperazineethanesulfonic acid
HOBt	1 <i>H</i> -1,2,3-benzotriazol-1-ol
HPLC	high performance liquid chromatography
HRMS	high resolution mass spectrometry
IPTG	isopropyl β-D-1-thiogalactopyranoside
LB	lysogeny broth
LCMS	liquid chromatography mass spectrometry
MBP	maltose binding protein

MES	2-(<i>N</i> -morpholino)ethanesulfonic acid
NHS	<i>N</i> -hydroxysuccinimide
NMR	nuclear magnetic resonance
NTA	nitrilotriacetic acid
Nle	norleucine
NS2B	non-structural protein 2B
NS3	non-structural protein 3
OD ₆₀₀	optical density at 600 nm
PAGE	polyacrylamide gel electrophoresis
pIII	minor coat protein
SDS	sodium dodecyl sulphate
SMILES	simplified molecular input line entry system
SOC	super optimal broth with catabolite repression
SPPS	solid-phase peptide synthesis
SPR	surface plasmon resonance
TCEP	tris(2-carboxyethyl)phosphine
TEV	tobacco etch virus
TFA	trifluoroacetic acid
TIPS	triisopropylsilane
Tris	2-amino-2-(hydroxymethyl)propane-1,3-diol
UV	ultraviolet light

Materials

Unless otherwise specified the materials used in this study were obtained commercially from Sigma-Aldrich (USA), Thermo Fisher Scientific (USA), AK Scientific (USA), Ambeed (USA) or Astral Scientific (Australia). Ultrapure water was produced in-house using a Milli-Q purification system (Millipore, USA).

Linear peptide synthesis

Linear peptides (**1a–8a**) were synthesised manually (**2a, 4a, 7a, 8a**) in fritted syringes (Torviq, USA) or using an Initiator+ Alstra (Biotage, Sweden) synthesiser (**1a, 3a, 5a, 6a**). Solid-phase synthesis was performed on Rink amide resin (GL Biochem, China) with a capacity of 0.6 mmol/g. Peptide synthesis reagents were used without purification from commercial sources: Fmoc-AA (GL Biochem, China; AK Scientific, USA; Ambeed, USA), coupling reagents (GL Biochem, China), solvents (ChemSupply, Australia), others (Sigma Aldrich, USA; AK Scientific, USA).

<i>Resin swelling</i>	CH ₂ Cl ₂ , 1 h.
<i>Standard wash</i>	DMA, CH ₂ Cl ₂ , DMF, 3× each (manual). DMF, 2–4× (automated).
<i>Fmoc deprotection</i>	Piperidine in DMF (20% v/v), 2× 5 min (manual). Piperidine in DMF (15% v/v), 1× 3 min, 1× 10 min. (automated).
<i>Amino acid coupling</i>	HBTU (3 eq), HOBt (3 eq), DIPEA (4 eq), Fmoc-AA (3 eq) in DMF, room temperature, 1–2× 1–2 h (manual). HBTU (2.5 eq), HOBt (2.5 eq), DIPEA (5 eq), Fmoc-AA (2.5 eq) in DMF, room temperature, 1–2× 1 h (automated).
<i>Final wash</i>	DMA, CH ₂ Cl ₂ , DMF, Et ₂ O, 3–5× each (manual). CH ₂ Cl ₂ , 6× (automated).
<i>Resin cleavage</i>	TFA, thioanisole, EDT, TIPS, water (86:5:3:3:3 v/v), 3–4 h.
<i>Work-up</i>	Precipitation of entire cleavage solution in ice-cold Et ₂ O. Centrifugation at 4500 × g, 5 min. Drying under vacuum for 1–2 h. Purification of crude product using preparative HPLC.

Supplementary Table 1. Linear peptide sequences synthesised for this study.

Compound	N-terminus	Sequence^[a]	C-terminus
1a	H-	<u>C</u> AYTN <u>C</u> G	-NH ₂
2a	H-	<u>C</u> HYLC	-NH ₂
3a	H-	<u>C</u> SDEV <u>C</u> W	-NH ₂
4a	H-	<u>c</u> PES <u>y</u> CA <u>K</u>	-NH ₂
5a	H-	<u>C</u> SHPQ <u>F</u> <u>C</u>	-NH ₂
6a	H-	<u>C</u> GKRK <u>S</u> <u>C</u> F	-NH ₂
7a	H-	<u>C</u> GSGY <u>G</u> SG <u>C</u>	-NH ₂
8a	H-	<u>C</u> IMAG <u>Y</u> <u>C</u>	-NH ₂
1a-C1A	H-	AAAYTN <u>C</u> G	-NH ₂
1a-C6A	H-	<u>C</u> AYTNAG	-NH ₂

[a] c = D-cysteine, Ξ = L-propargylglycine, y = D-tyrosine.

HPLC purification

Peptides (**1a-8a**, **1b-8b**, **4c**) underwent purification on a 2695 Separations Module (Waters, USA) by preparative reverse phase HPLC at 5 mL/min flow using column A, monitoring 214 nm, 254 nm and 270 nm wavelengths on a 2996 Photodiode Array Detector (Waters, USA). Isolated fractions were lyophilised using an Alpha 1-2 freeze dryer (Christ, Germany).

Solvent system A ultrapure H₂O (solvent 1), HPLC-grade acetonitrile (solvent 2)
0.1% v/v trifluoroacetic acid additive in both solvents

Solvent system B ultrapure H₂O (solvent 1), HPLC-grade acetonitrile (solvent 2)
0.1% v/v formic acid additive in both solvents

Column A SymmetryPrep C₁₈, 19 mm × 150 mm, 7 μm (Waters, USA)

Method A This purification employed solvent system 1. The method started at 5% solvent 2 in solvent 1 and this percentage was held until minute 2. The proportion of solvent 2 was increased gradually up to 90% at minute 22. This percentage was held until minute 60. This method was used for the purification of compounds **1a**, **1a-C1A**, **1a-C6A**, **4a**, **5a**, **6a**.

Method B This purification employed solvent system 1. The method started at 5% solvent 2 in solvent 1 and this percentage was held until minute 2. The proportion of solvent 2 was increased gradually up to 60% at minute 22. This percentage was held until minute 60. This method was used for the purification of compounds **2a**, **7a** and **8a**.

Method C This purification employed solvent system 2. The method started at 5% solvent 2 in solvent 1 and this percentage was held until minute 2. The proportion of solvent 2 was increased gradually up to 60% at minute 22. This percentage was held until minute 60. This method was used for the purification of compound **1b**.

Method D This purification employed solvent system 2. The method started at 5% solvent 2 in solvent 1 and this percentage was held until minute 2. The proportion of solvent 2 was increased gradually up to 60% at minute 42. This percentage was held until minute 60. This method was used for the purification of compound **6b**.

Method E This purification employed solvent system 2. The method started at 5% solvent 2 in solvent 1 and this percentage was held until minute 2. The proportion of solvent 2 was increased gradually up to 60% at minute 62. This percentage was held until minute 90. This method was used for the purification of compound **3a**.

Method F This purification employed solvent system 2. The method started at 5% solvent 2 in solvent 1 and this percentage was held until minute 2. The proportion of solvent 2 was increased gradually up to 40% at minute 57. This percentage was held until minute 60. This method was used for the purification of compounds **2b, 3b, 4b, 4c, 5b** and **7b**.

Method G This purification employed solvent system 2. The method started at 5% solvent 2 in solvent 1 and this percentage was held until minute 2. The proportion of solvent 2 was increased gradually up to 90% at minute 22. This percentage was held until minute 60. This method was used for the purification of compound **8b**.

LCMS analysis

The analytical reverse phase LCMS system 1260/6120 (Agilent, USA) was used to monitor reaction mixtures and purified peptide products using UV detection and ESI+ spectrometry.

Solvent system C ultrapure H₂O (solvent 1), LCMS-grade acetonitrile (solvent 2)
0.1% v/v formic acid additive in both solvents

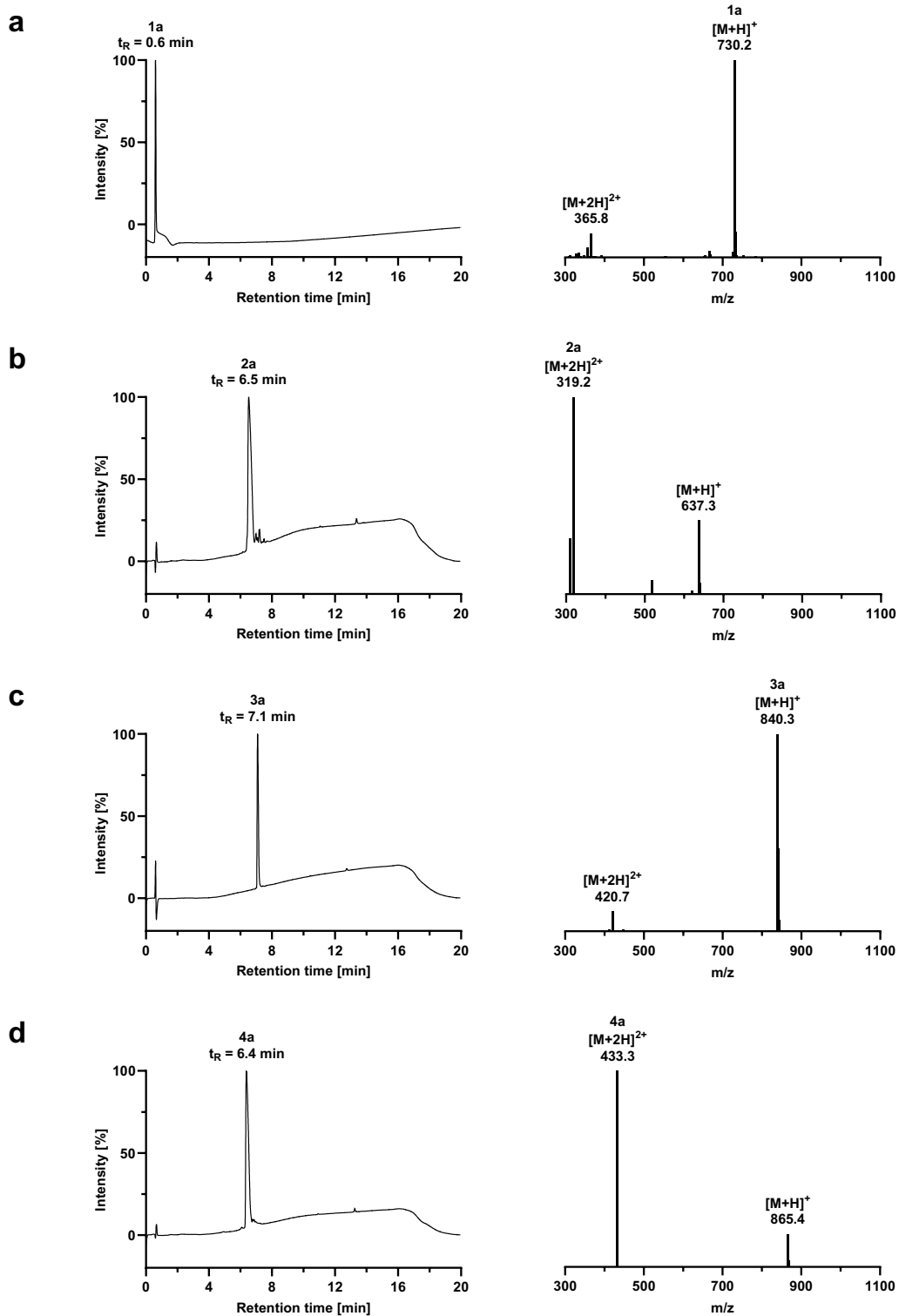
Column B Poroshell 120, EC-C₁₈, 3.0 mm × 50 mm, 2.7 μm (Agilent, USA)

Column C Alltima HP C₁₈-AQ, 2.1 mm × 150 mm, 5 μm (VWR, USA)

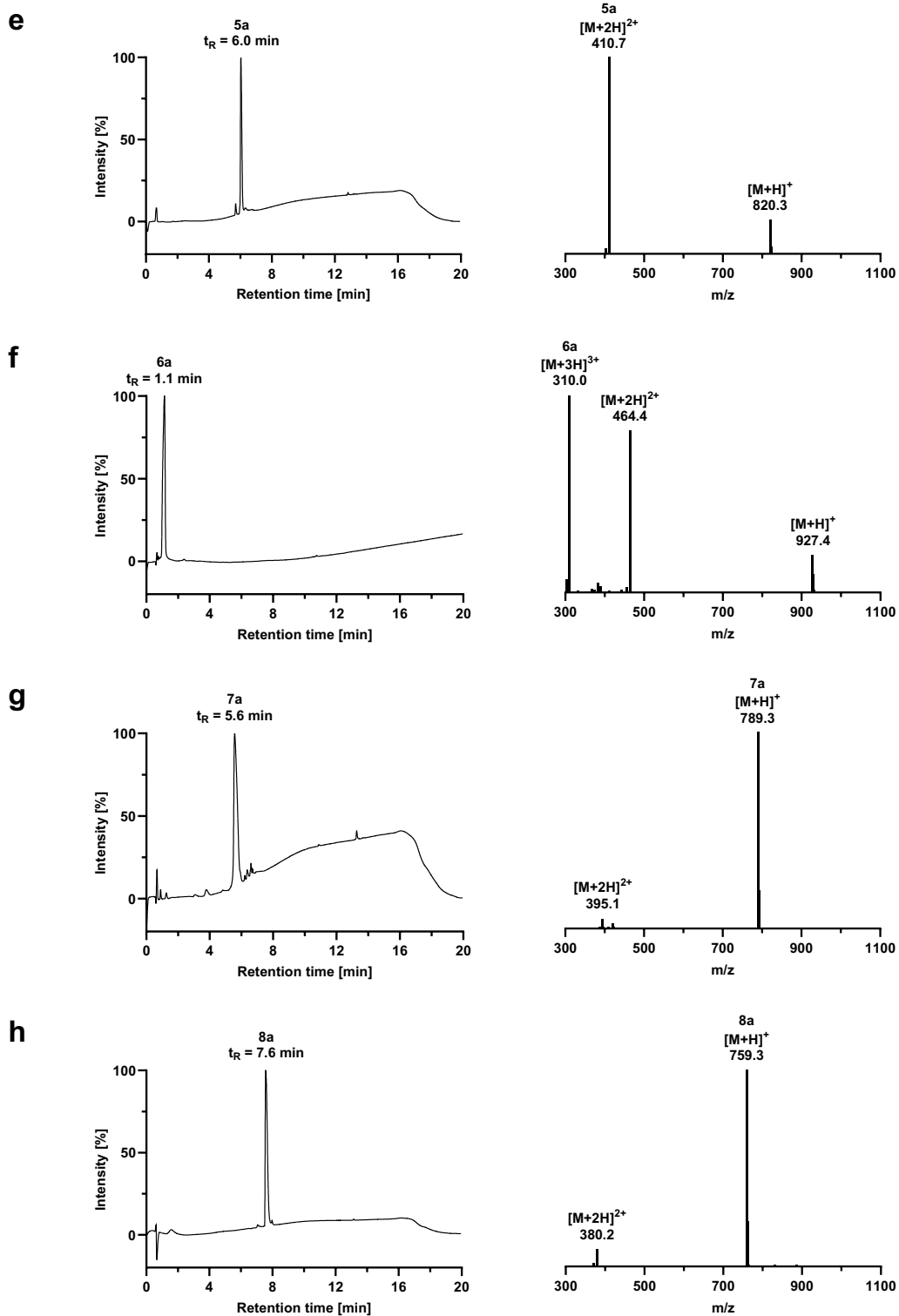
Method H This analysis employed solvent system C at 0.3 mL/min flow using column B. The method started at 5% solvent 2 in solvent 1. The proportion of solvent 2 was increased gradually up to 90% at minute 10. This percentage was held until minute 13. The proportion of solvent 2 was decreased gradually down to 5% at minute 14. This percentage was held until minute 20.

Method I This analysis employed solvent system C at 1.0 mL/min flow using column C. The method started at 100% solvent 1. The proportion of solvent 2 in solvent 1 was increased gradually up to 30% at minute 30. This percentage was held until minute 35.

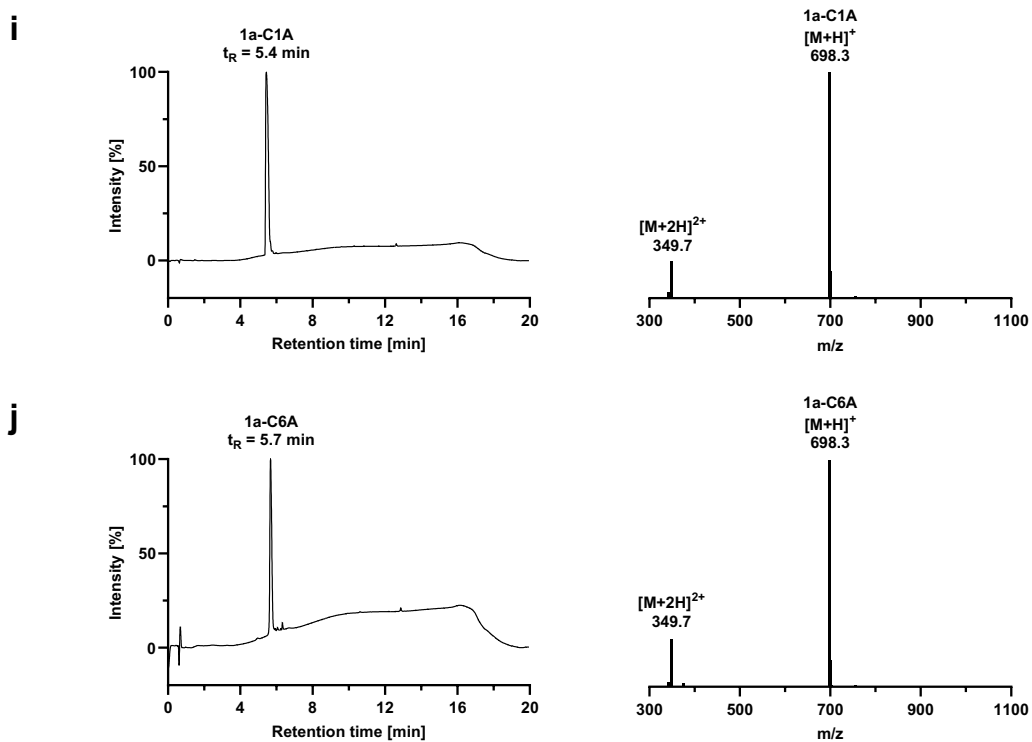
Method J This analysis employed solvent system C at 0.3 mL/min flow using column B. The method started at 5% solvent 2 in solvent 1. The proportion of solvent 2 in solvent 1 was increased gradually up to 60% at minute 22. This percentage was held until minute 22.2. The proportion of solvent 2 was decreased gradually down to 5% at minute 22.5. This percentage was held until minute 25.



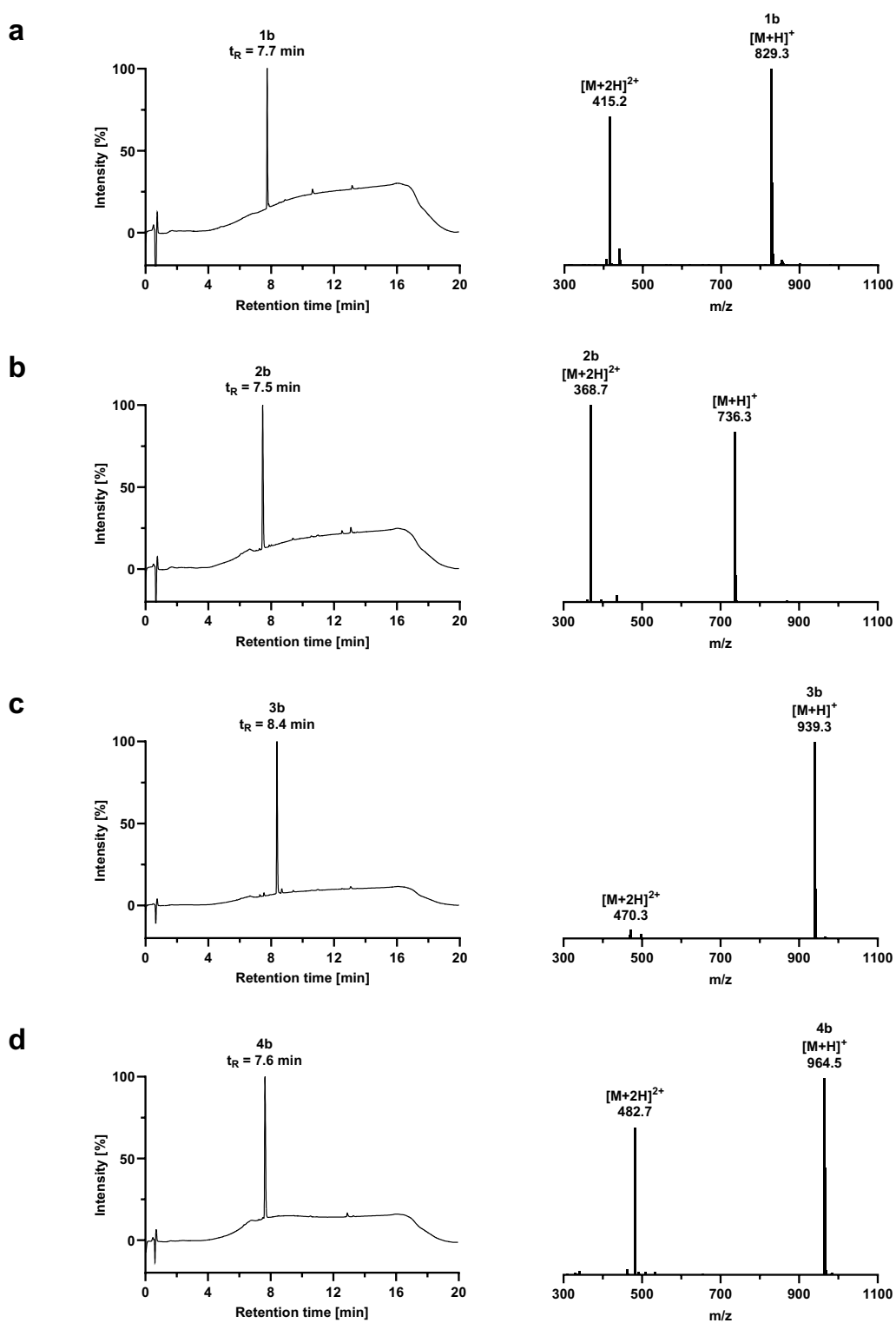
Supplementary Figure 1. (continued)



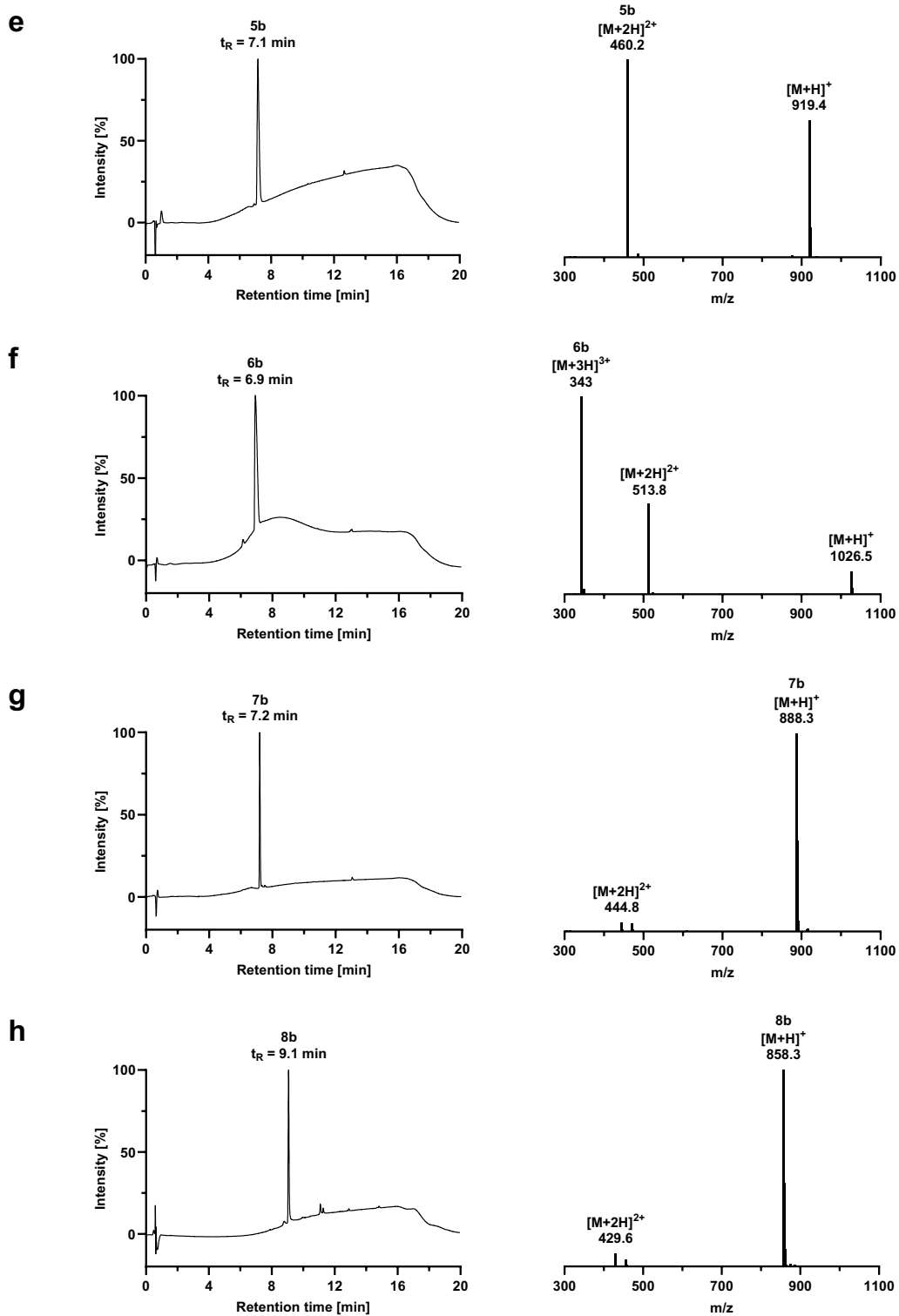
Supplementary Figure 1. (continued)



Supplementary Figure 1. LCMS traces (214 nm) and spectra (ESI⁺) of purified linear peptides **1a–8a** and alanine mutants **1a-C1A** and **1a-C6A**. (a) **1a** (method J), (b) **2a** (method H), (c) **3a** (method H), (d) **4a** (method H), (e) **5a** (method H), (f) **6a** (method J), (g) **7a** (method H), (h) **8a** (method H), (i) **1a-C1A** (method H), (j) **1a-C6A** (method H).



Supplementary Figure 2. (continued)



Supplementary Figure 2. LCMS traces (214 nm) and spectra (ESI+) of purified stapled peptides **1b–8b** (method H). (a) **1b**, (b) **2b**, (c) **3b**, (d) **4b**, (e) **5b**, (f) **6b**, (g) **7b**, (g) **8b** (254 nm).

Peptide stapling

Purified linear peptide (**1a-8a**) was exposed to 1.2 eq of stapling reagent (2-chloromethyl-6-cyanopyridine, **10**; Ambeed, USA) from a concentrated acetonitrile stock at 1 mM in aqueous buffer (20 mM Tris-HCl pH 7.4, 1 mM TCEP) at room temperature for 20 h to give the stapled peptide products (**1b-8b**). The resulting peptide macrocycles were purified by preparative HPLC.

Buffer and concentration variations

In addition to the general condition using physiological pH, the peptide stapling reaction with purified linear peptide **1a** was performed using alternative buffer compositions to test slightly acidic (20 mM MES pH 6.5, 1 mM TCEP) and basic (20 mM HEPES-KOH pH 8.0, 1 mM TCEP) reaction environments. Furthermore, instead of at 1 mM, the peptide stapling reaction was also tested using 100 μ M and 5 mM of purified linear peptide **1a** as starting material.

Stapling kinetics

The peptide stapling reactions were monitored using LCMS method H. Aliquots of the reactions were quenched by the addition of formic acid to 0.1% v/v at 1.5, 3, 16 and 20 h after addition of the stapling reagent. Percent conversion was determined through integration of the peaks of the starting material, product and byproducts at 280 nm. Data were plotted and analysed using GraphPad Prism 10 (Dotmatics, USA) applying a time-dependent saturation equation (**Supplementary Equation 1**).

Supplementary Equation 1.

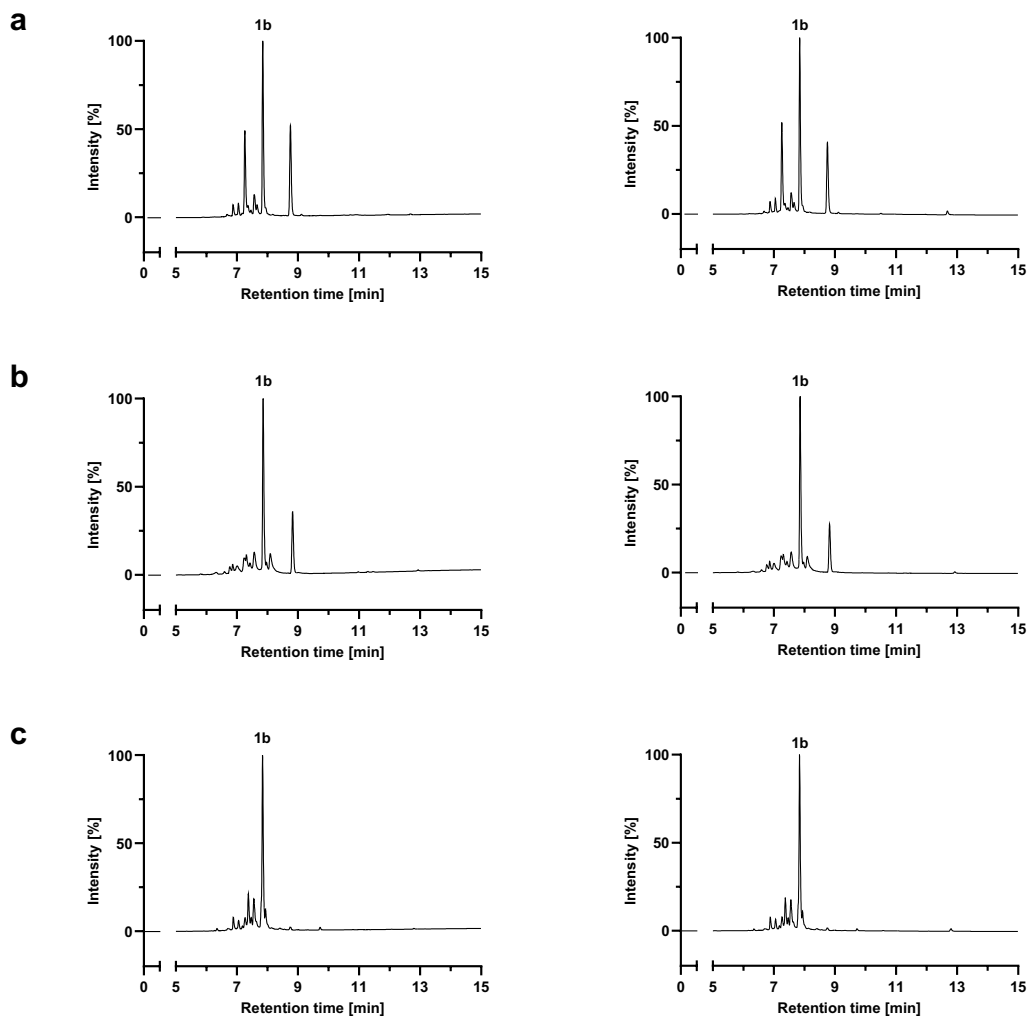
$$Y = \frac{P_{max} \cdot \frac{1}{t_{half}} \cdot X}{1 + \frac{1}{t_{half}} \cdot X}$$

Y = product [%]

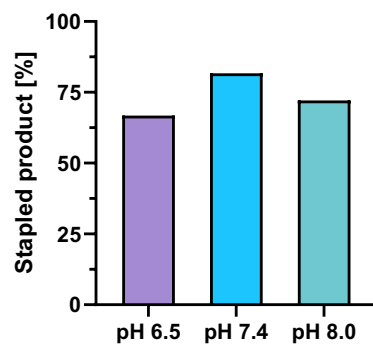
P_{max} = maximum product [%]

t_{half} = half-time of formation [min]

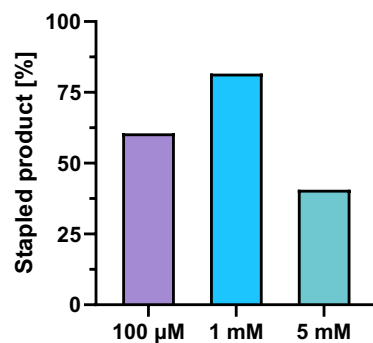
X = time [min]



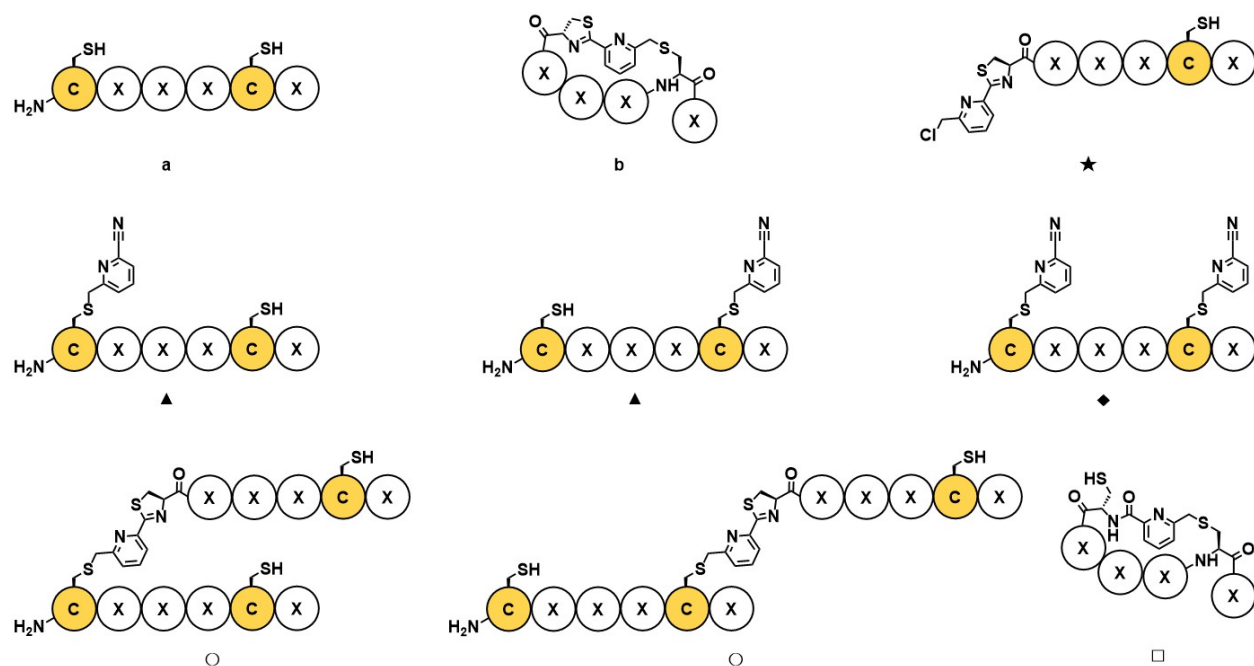
Supplementary Figure 3. LCMS traces (left: 254 nm, right: 280 nm) of stapling reactions with purified linear peptide **1a** at (a) pH 6.5, (b) pH 7.4 and (c) pH 8.0 (all method H).



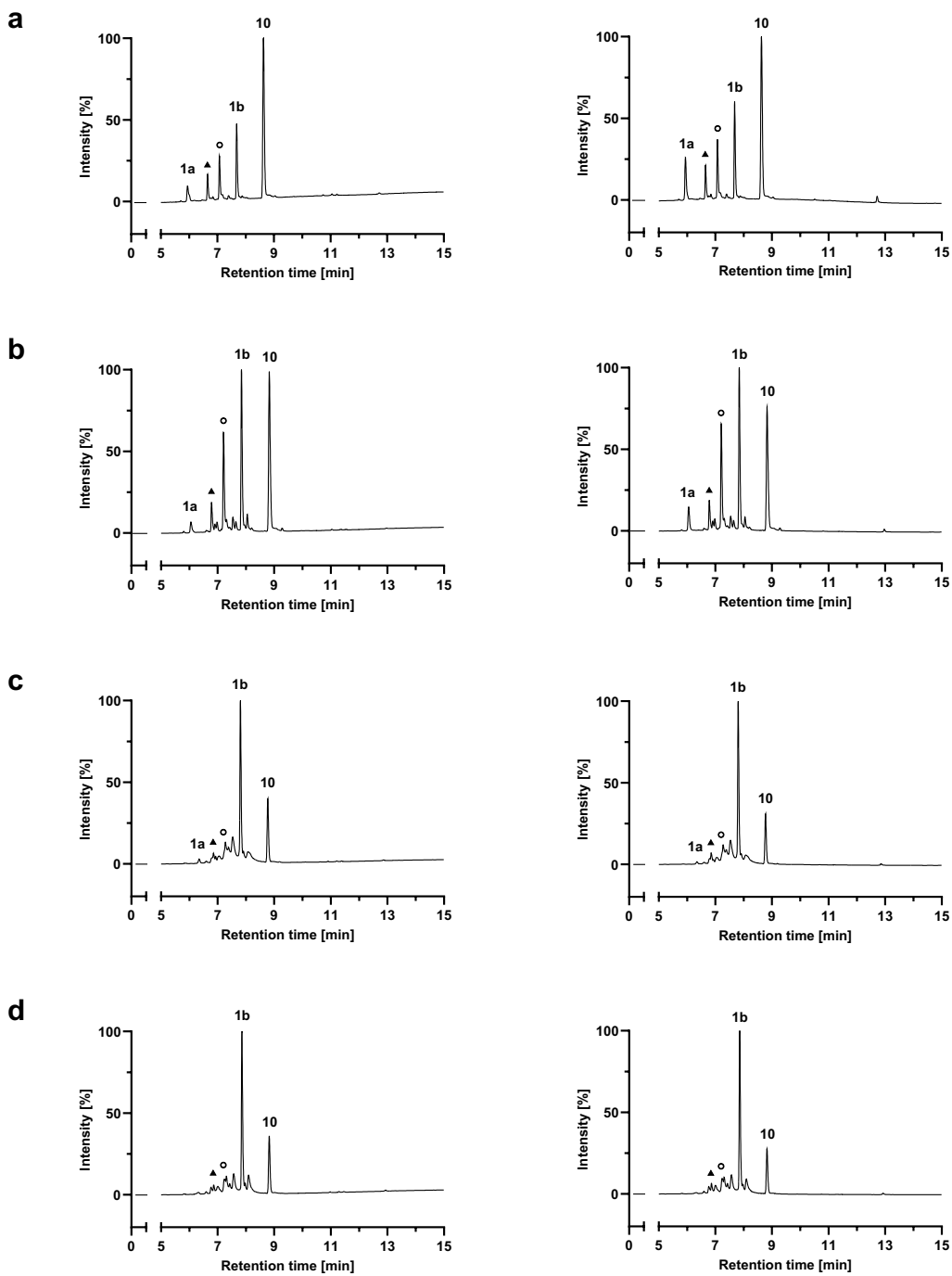
Supplementary Figure 4. Conversion of purified linear peptide **1a** into stapled peptide **1b** based on LCMS traces (280 nm) at pH 6.5 (purple), pH 7.4 (blue) and pH 8.0 (green).



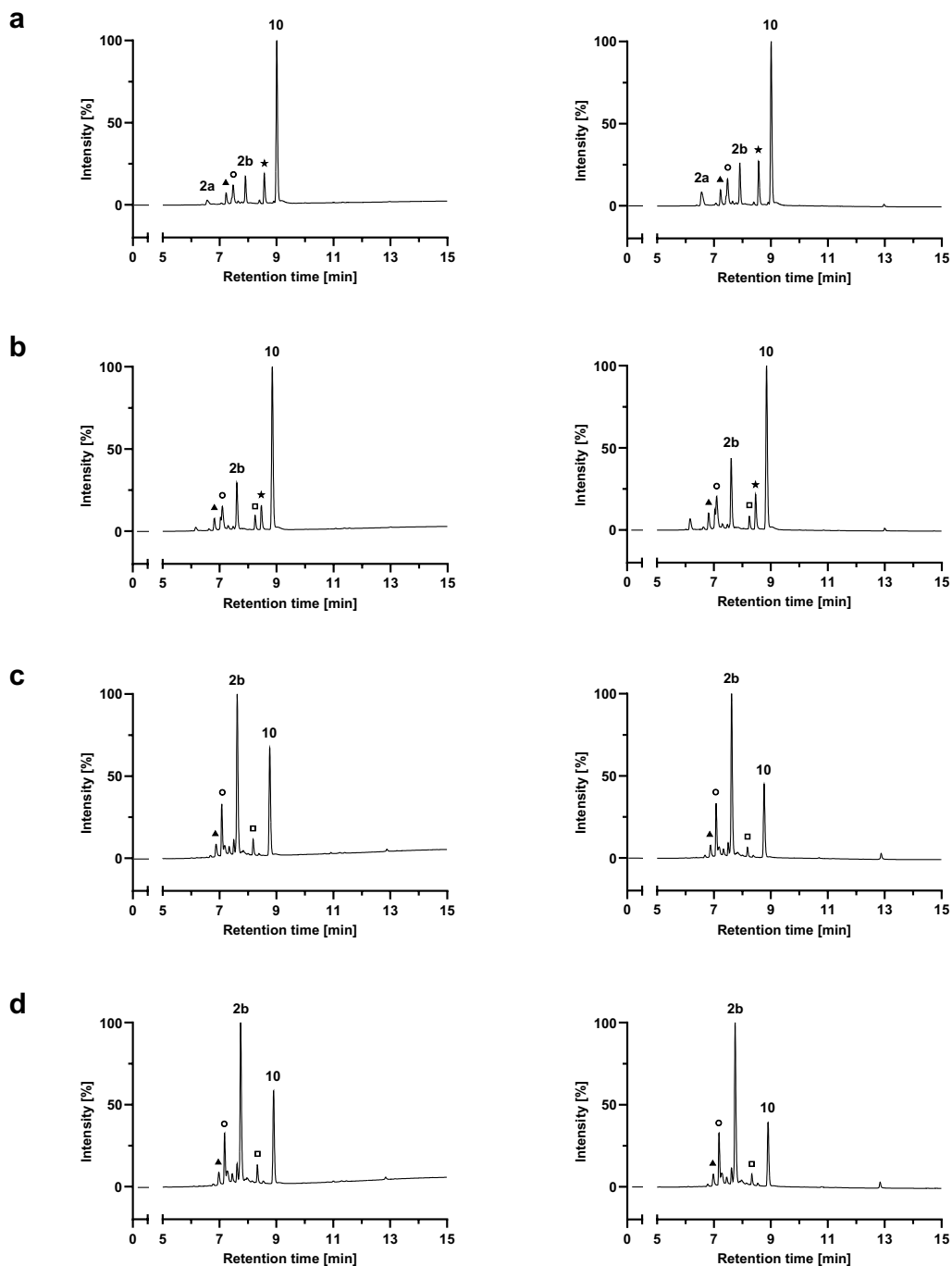
Supplementary Figure 5. Conversion of purified linear peptide **1a** into stapled peptide **1b** based on LCMS traces (280 nm) using different starting material concentrations: 100 μM (purple), 1 mM (blue) and 5 mM (green).



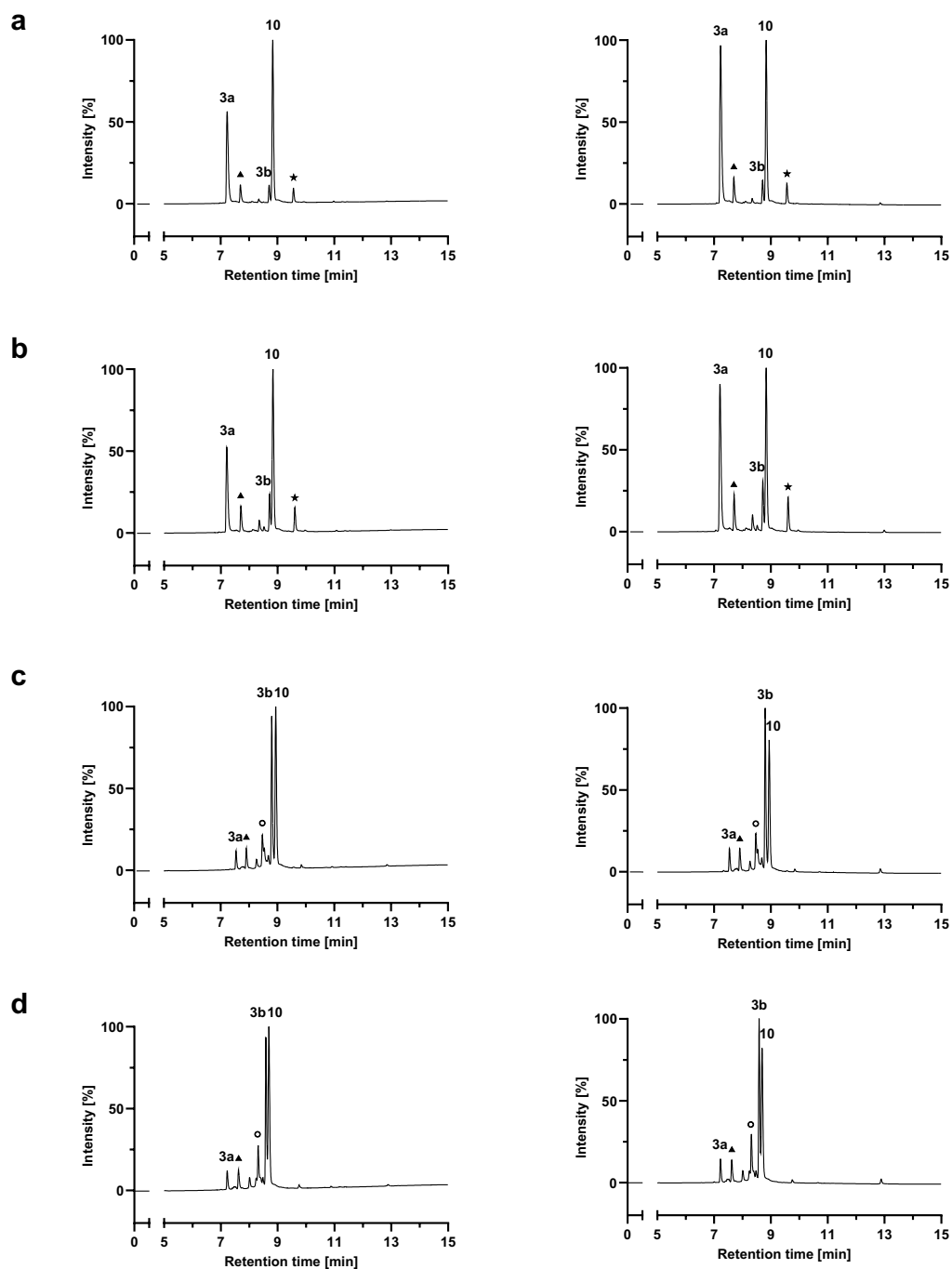
Supplementary Figure 6. Legend for the following LCMS data, showing cartoon representations of starting materials (a), desired products (b), and proposed byproducts (★, ▲, ◆, ○, □) of the stapling reaction. Peak labels were assigned through corresponding ESI+ MS data.



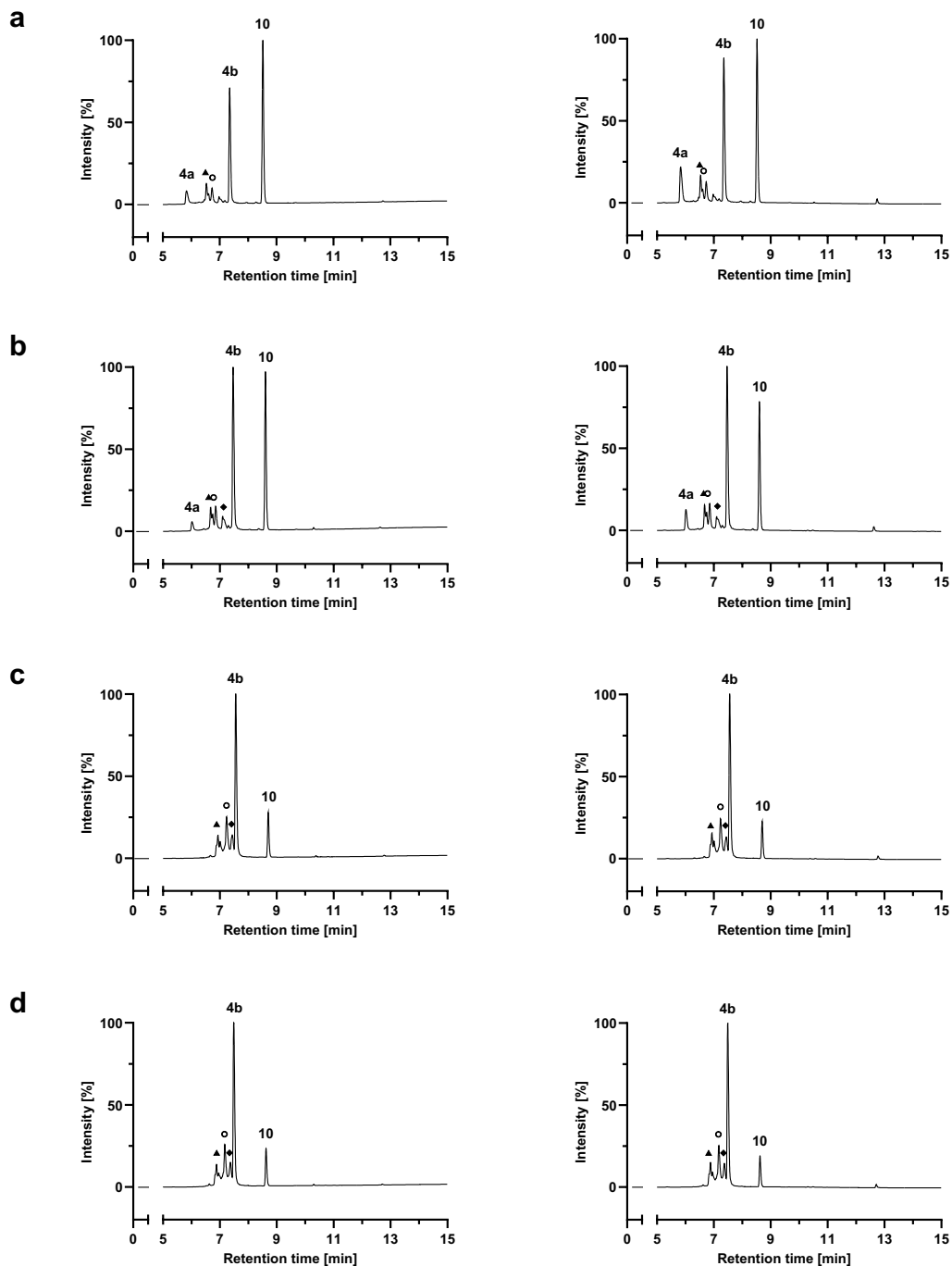
Supplementary Figure 7. LCMS traces (left: 254 nm, right: 280 nm) of stapling reactions of purified linear peptide **1a** resulting in stapled product **1b** after (a) 1.5 h, (b) 3 h, (c) 16 h, (d) 20 h (all method H).



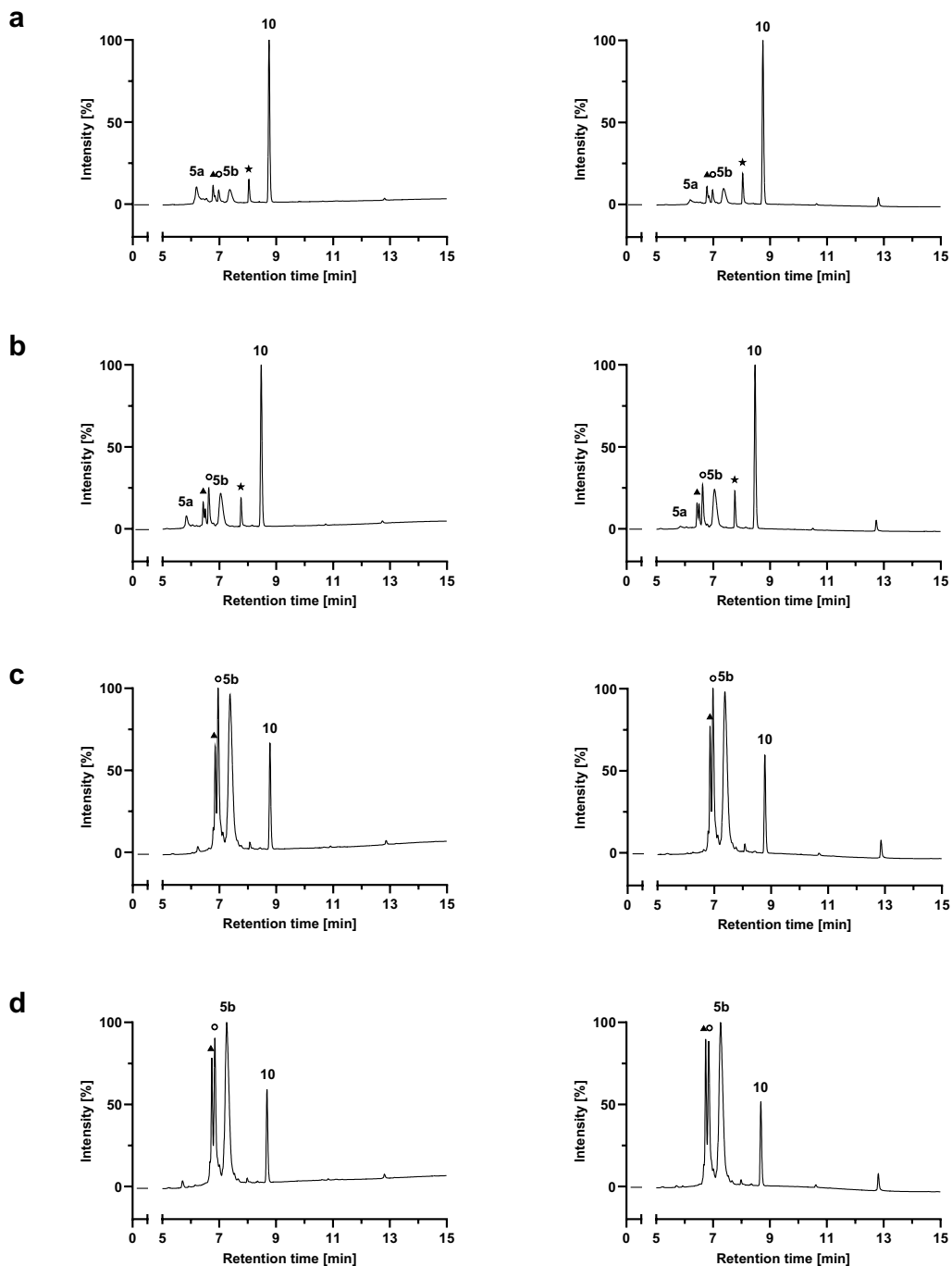
Supplementary Figure 8. LCMS traces (left: 254 nm, right: 280 nm) of stapling reactions of purified linear peptide **2a** resulting in stapled product **2b** after (a) 1.5 h, (b) 3 h, (c) 16 h, (d) 20 h (all method H).



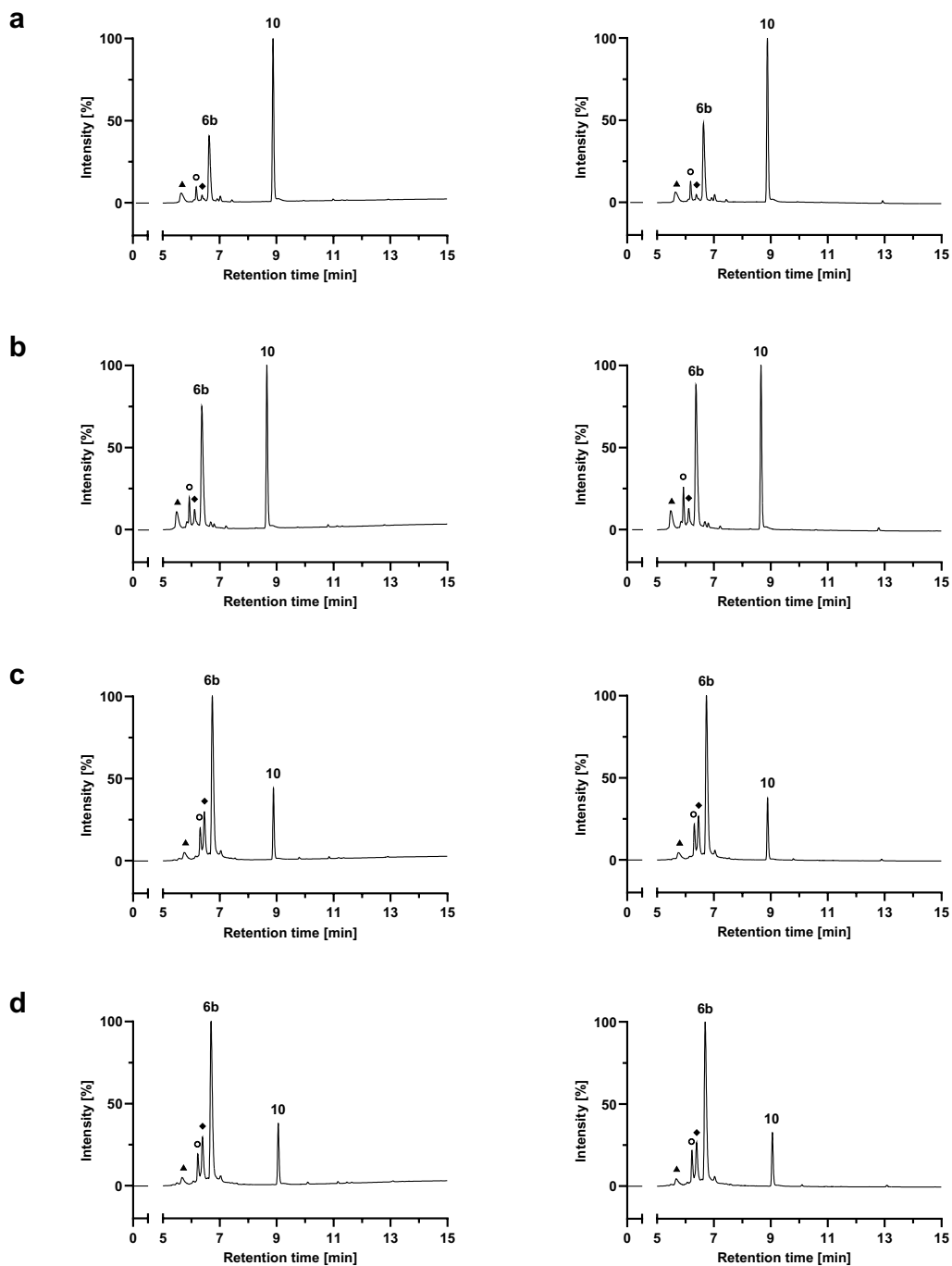
Supplementary Figure 9. LCMS traces (left: 254 nm, right: 280 nm) of stapling reactions of purified linear peptide **3a** resulting in stapled product **3b** after (a) 1.5 h, (b) 3 h, (c) 16 h, (d) 20 h (all method H).



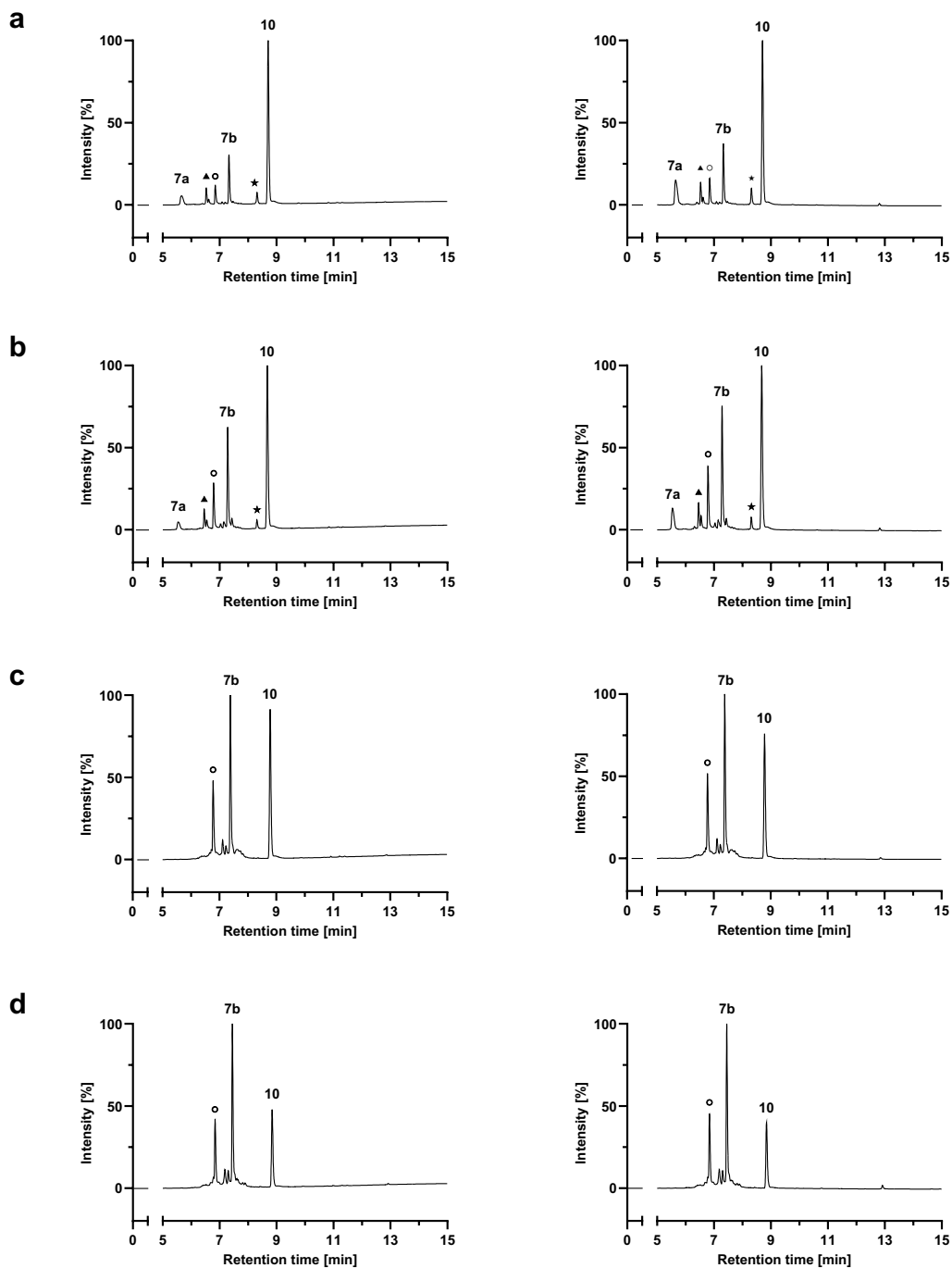
Supplementary Figure 10. LCMS traces (left: 254 nm, right: 280 nm) of stapling reactions of purified linear peptide **4a** resulting in stapled product **4b** after (a) 1.5 h, (b) 3 h, (c) 16 h, (d) 20 h (all method H).



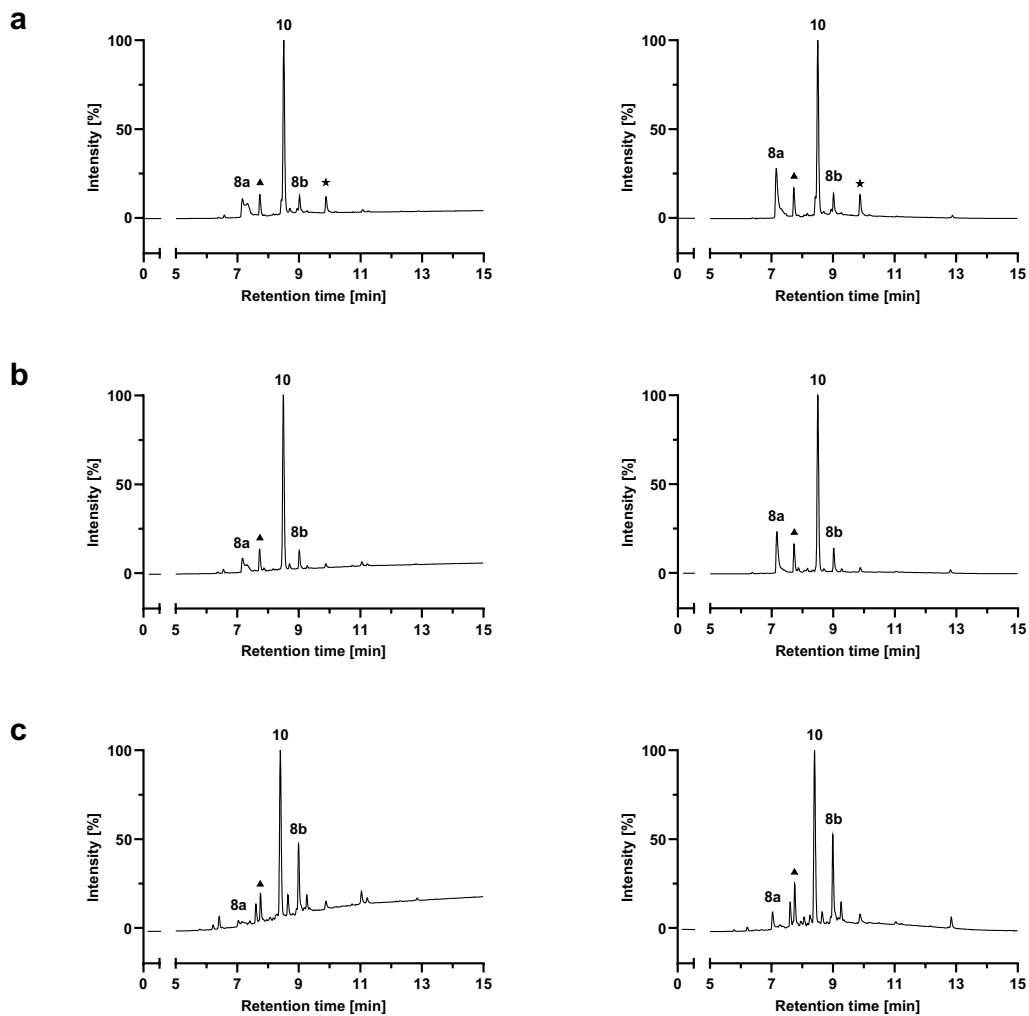
Supplementary Figure 11. LCMS traces (left: 254 nm, right: 280 nm) of stapling reactions of purified linear peptide **5a** resulting in stapled product **5b** after (a) 1.5 h, (b) 3 h, (c) 16 h, (d) 20 h (all method H).



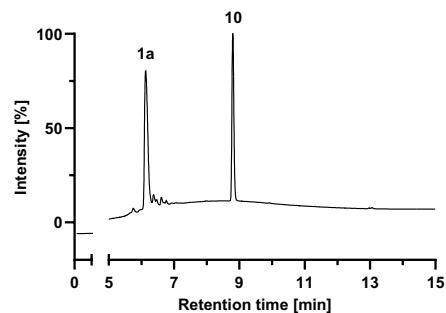
Supplementary Figure 12. LCMS traces (left: 254 nm, right: 280 nm) of stapling reactions of purified linear peptide **6a** resulting in stapled product **6b** after (a) 1.5 h, (b) 3 h, (c) 16 h, (d) 20 h (all method H).



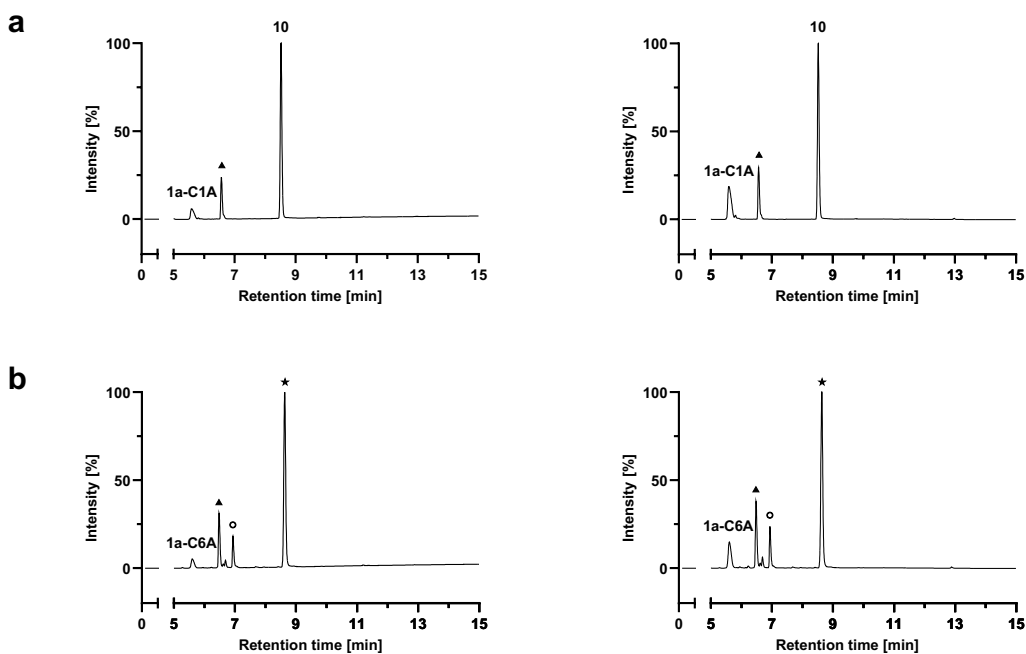
Supplementary Figure 13. LCMS traces (left: 254 nm, right: 280 nm) of stapling reactions of purified linear peptide **7a** resulting in stapled product **7b** after (a) 1.5 h, (b) 3 h, (c) 16 h, (d) 20 h (all method H).



Supplementary Figure 14. LCMS traces (left: 254 nm, right: 280 nm) of stapling reactions of purified linear peptide **8a** resulting in stapled product **8b** after (a) 1.5 h, (b) 3 h, (c) 20 h (all method H).



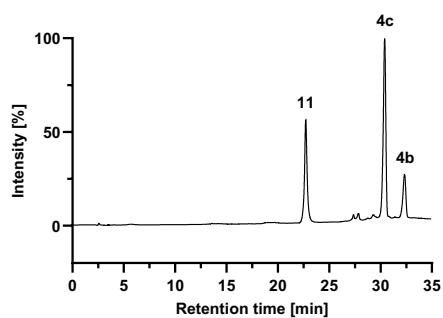
Supplementary Figure 15. LCMS trace (214 nm) of **1a** and **10** in 20 mM Tris-HCl pH 7.4, 1 mM TCEP containing 0.1% v/v formic acid after 90 min, showing the reaction is stopped in acidic pH.



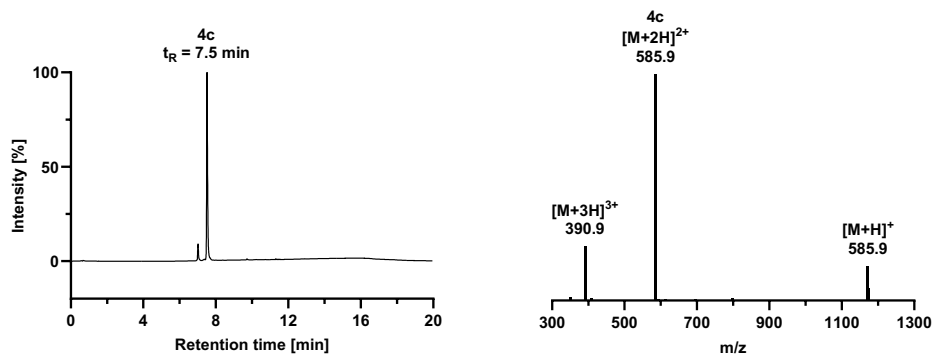
Supplementary Figure 16. LCMS traces (left: 254 nm, right: 280 nm) of reactions of alanine mutants (a) **1a-C1A** or (b) **1a-C6A** with **10** after 90 min.

Azide-alkyne cycloaddition

This protocol was inspired by previous research by Bell & Malins.¹ Purified alkyne-containing stapled peptide (**4b**) was exposed to 1.2 eq of 4-azido-L-phenylalanine (**11**; Chem Impex, USA) at 1 mM in presence of 0.6 eq of CuSO₄, 0.6 eq of BTAA and 0.6 eq of sodium ascorbate in aqueous buffer (20 mM Tris-HCl pH 7.4) at room temperature for 24 h to give compound **4c**. The reaction was analysed by LCMS using method I. Compound **4c** was purified by preparative HPLC.



Supplementary Figure 17. LCMS trace (254 nm) of click reaction mixture of purified stapled peptide **4b** with azide **11** yielding click product **4c** (method I).



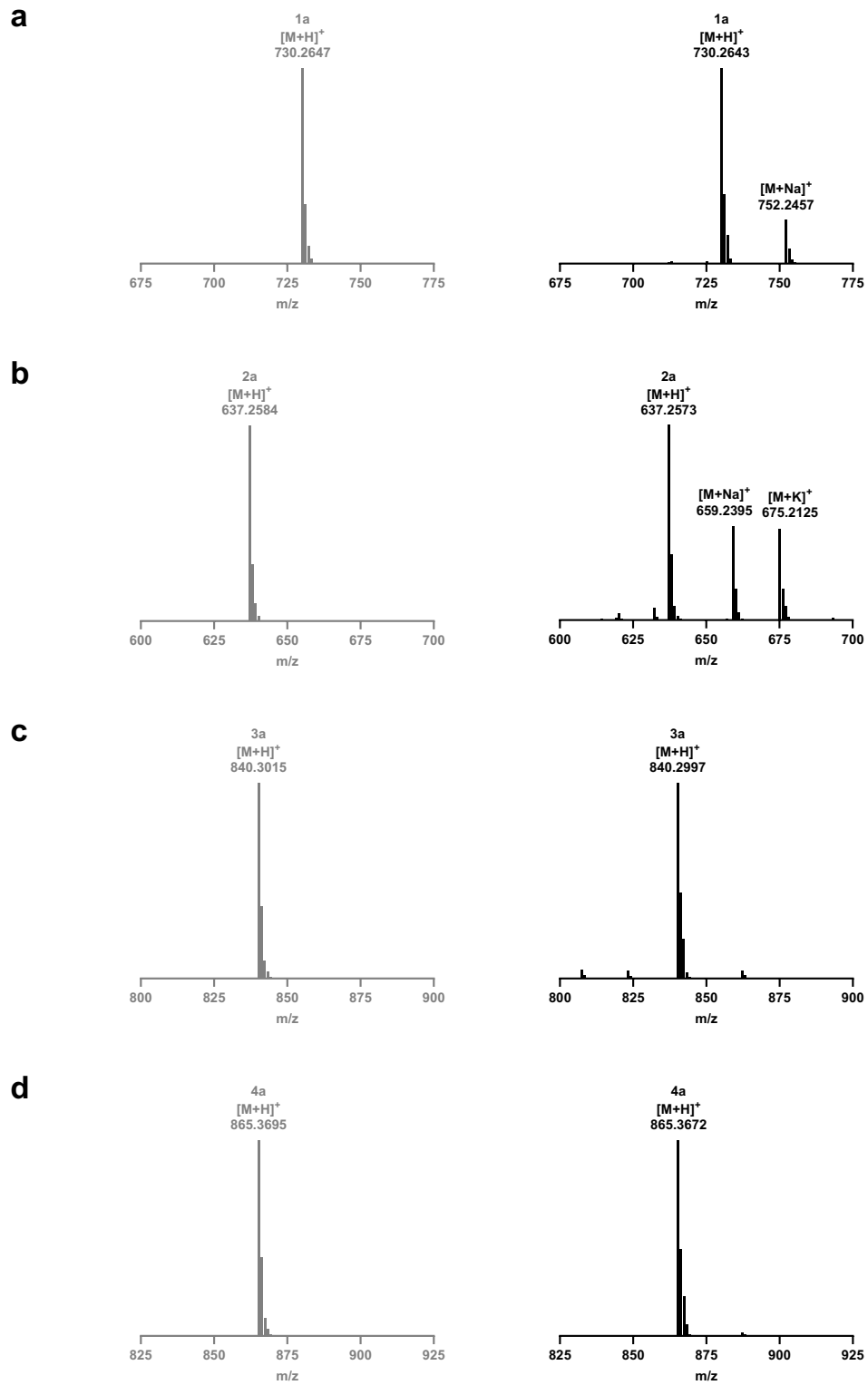
Supplementary Figure 18. LCMS trace (254 nm) and spectrum (ESI+) of purified click product **4c** (method H).

HRMS analysis

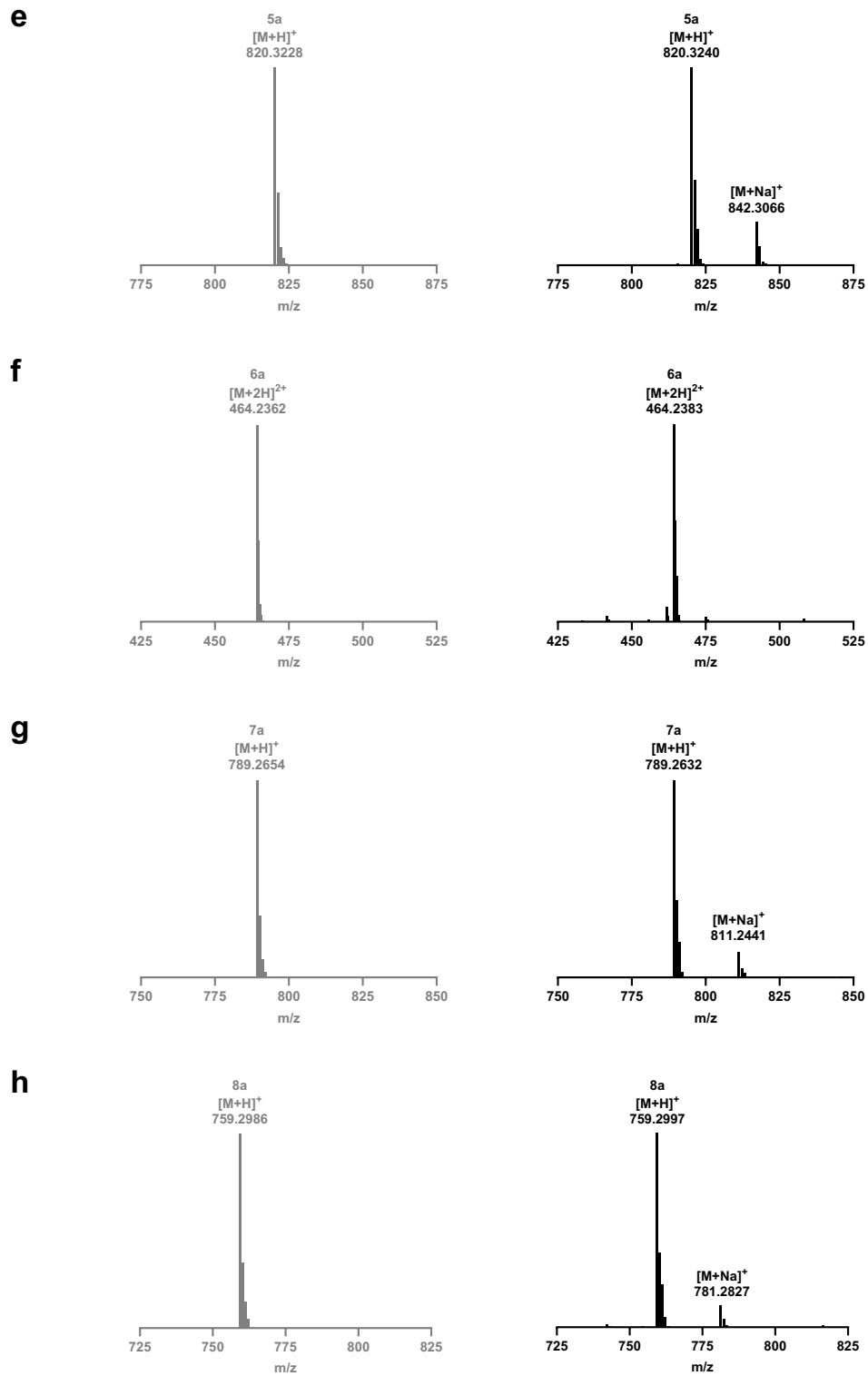
The identity of linear and stapled peptides was confirmed using high-resolution ESI+ mass spectrometry with an Orbitrap Elite mass spectrometer (Thermo Fisher Scientific, USA). The anticipated mass-to-charge ratios and isotope patterns were calculated with enviPat Web² (Eawag, Switzerland).

Supplementary Table 2. High-resolution mass spectrometry characterisation of created peptides.

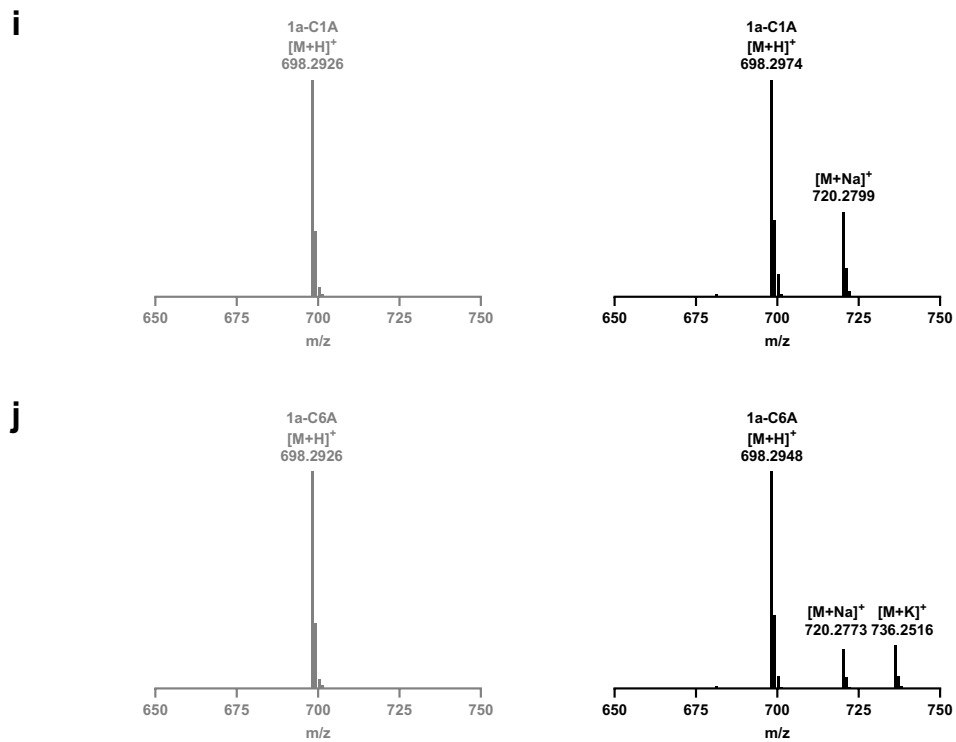
Compound	Molecular formula	Ion	Calculated	Observed
1a	C ₂₈ H ₄₃ N ₉ O ₁₀ S ₂	[M+H] ⁺	730.2647	730.2643
1b	C ₃₅ H ₄₄ N ₁₀ O ₁₀ S ₂	[M+Na] ⁺	851.2576	851.2559
2a	C ₂₇ H ₄₀ N ₈ O ₆ S ₂	[M+H] ⁺	637.2584	637.2573
2b	C ₃₄ H ₄₁ N ₉ O ₆ S ₂	[M+Na] ⁺	758.2513	758.2481
3a	C ₃₄ H ₄₉ N ₉ O ₁₂ S ₂	[M+H] ⁺	840.3015	840.2997
3b	C ₄₁ H ₅₀ N ₁₀ O ₁₂ S ₂	[M+Na] ⁺	961.2943	961.2931
4a	C ₃₇ H ₅₆ N ₁₀ O ₁₀ S ₂	[M+H] ⁺	865.3695	865.3672
4b	C ₄₄ H ₅₇ N ₁₁ O ₁₀ S ₂	[M+Na] ⁺	986.3623	986.3603
4c	C ₅₃ H ₆₇ N ₁₅ O ₁₂ S ₂	[M+H] ⁺	1170.4607	1170.4590
5a	C ₃₄ H ₄₉ N ₁₁ O ₉ S ₂	[M+H] ⁺	820.3228	820.3240
5b	C ₄₁ H ₅₀ N ₁₂ O ₉ S ₂	[M+H] ⁺	919.3337	919.3318
6a	C ₃₈ H ₆₆ N ₁₄ O ₉ S ₂	[M+2H] ²⁺	464.2362	464.2383
6b	C ₄₅ H ₆₇ N ₁₅ O ₉ S ₂	[M+2H] ²⁺	513.7416	513.7414
7a	C ₂₉ H ₄₄ N ₁₀ O ₁₂ S ₂	[M+H] ⁺	789.2654	789.2632
7b	C ₃₆ H ₄₅ N ₁₁ O ₁₂ S ₂	[M+Na] ⁺	910.2582	910.2549
8a	C ₃₁ H ₅₀ N ₈ O ₈ S ₃	[M+H] ⁺	759.2986	759.2997
8b	C ₃₈ H ₅₁ N ₉ O ₈ S ₃	[M+Na] ⁺	880.2915	880.2945
1a-C1A	C ₂₈ H ₄₃ N ₉ O ₁₀ S ₁	[M+H] ⁺	698.2926	698.2974
1a-C6A	C ₂₈ H ₄₃ N ₉ O ₁₀ S ₁	[M+H] ⁺	698.2926	698.2948



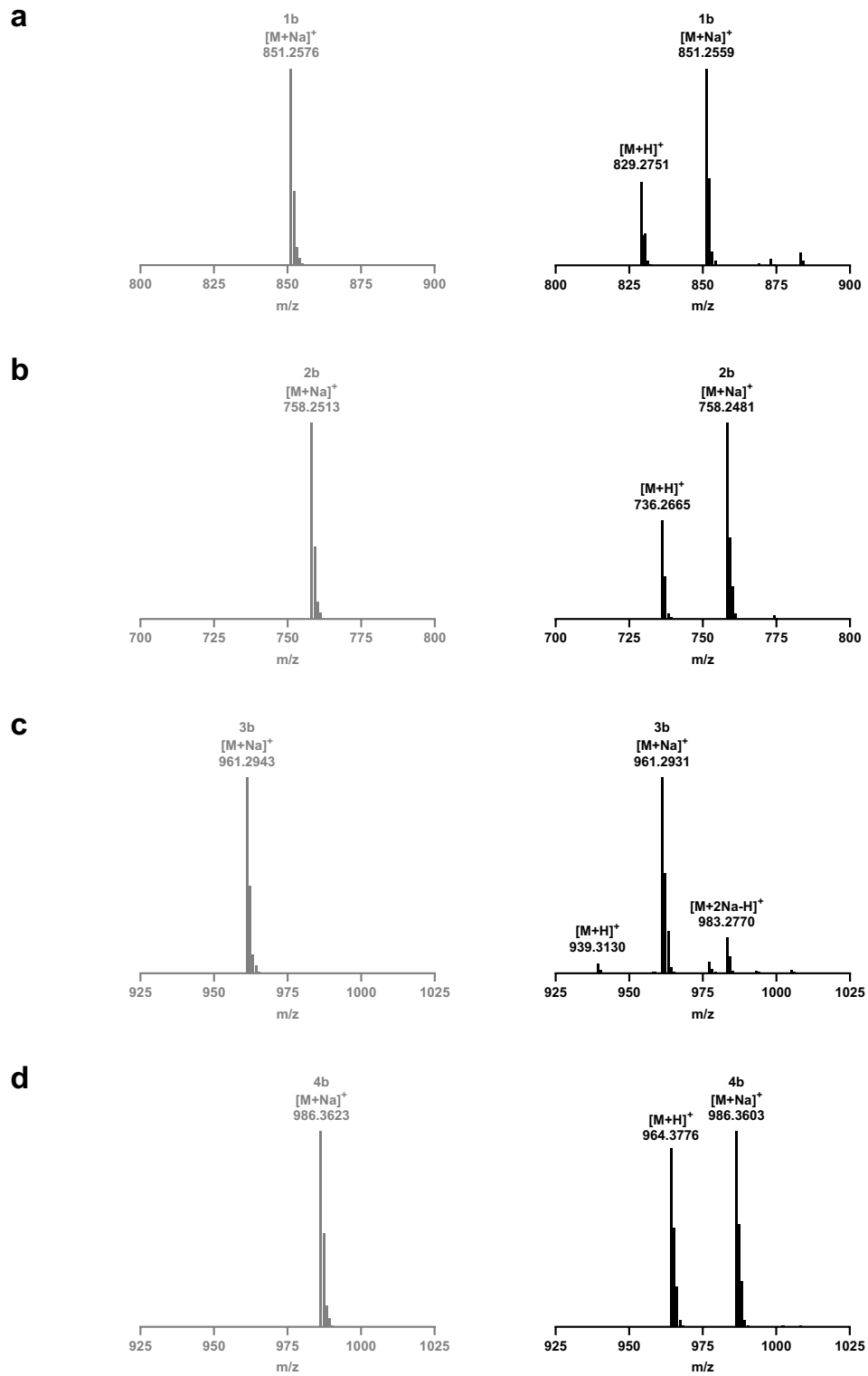
Supplementary Figure 19. (continued)



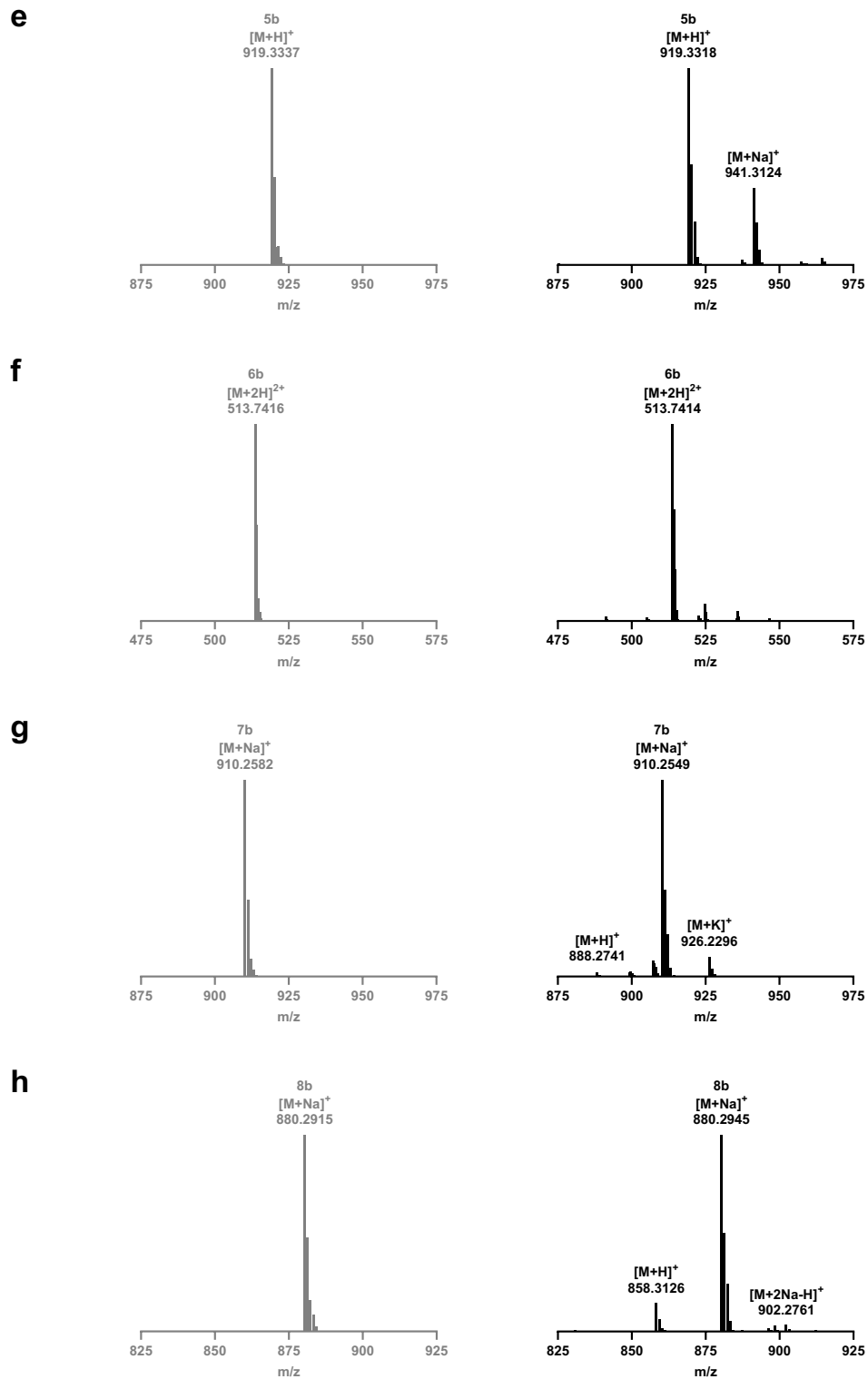
Supplementary Figure 19. (continued)



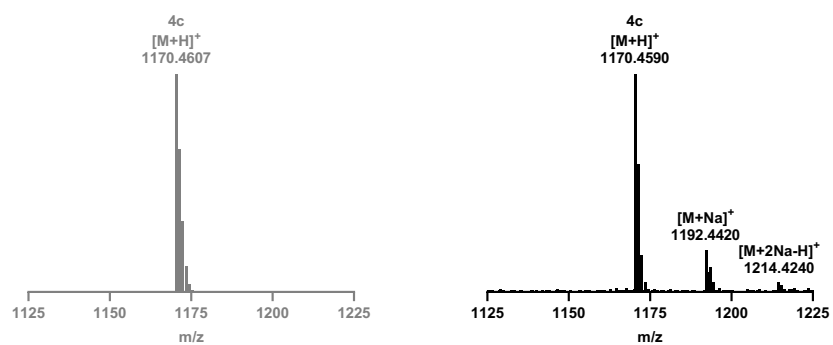
Supplementary Figure 19. Simulated isotope patterns (grey, left) and high-resolution mass spectra (black, right) of linear peptides (a) **1a**, (b) **2a**, (c) **3a**, (d) **4a**, (e) **5a**, (f) **6a**, (g) **7a**, (h) **8a**, (i) **1a-C1A**, (j) **1a-C6A**.



Supplementary Figure 20. (continued)



Supplementary Figure 20. Simulated isotope patterns (grey, left) and high-resolution mass spectra (black, right) of stapled peptides (a) **1b**, (b) **2b**, (c) **3b**, (d) **4b**, (e) **5b**, (f) **6b**, (g) **7b**, (h) **8b**.



Supplementary Figure 21. Simulated isotope pattern (grey, left) and high-resolution mass spectrum (black, right) of click reaction product **4c**.

SPR analysis

This protocol was adapted from previous research.³ SPR experiments were performed on a Biacore 8K (Cytiva, USA). Streptavidin (100 µg in 10 mM sodium acetate pH 3.9; New England Biolabs, USA) was immobilised on a CM5 chip (Cytiva, USA) by EDC/NHS bioconjugation using an amide coupling kit (Cytiva, USA) in absence of TCEP. Measurements using peptides **5a** and **5b** were carried out at 20 °C in single-cycle kinetics mode using an aqueous running buffer (20 mM HEPES-KOH pH 7.4, 150 mM NaCl, 0.5 mM TCEP, 0.05% v/v polysorbate 20). The instrument was operated using Biacore Insight 5 software (Cytiva, USA). Obtained data were plotted and analysed in GraphPad Prism 10 (Dotmatics, USA) using the non-linear fit ‘one site – specific binding’ (**Supplementary Equation 2**), with K_D values reported as calculated by this evaluation.

Supplementary Equation 2.

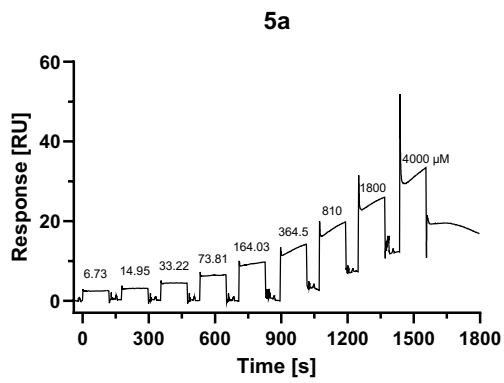
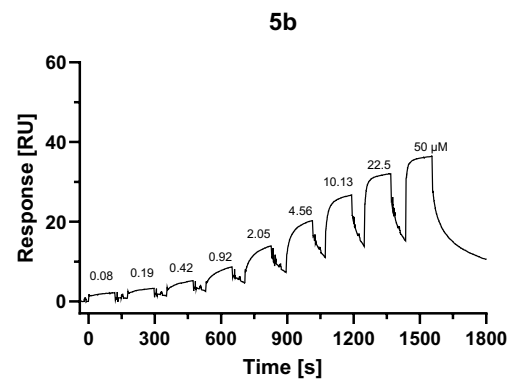
$$Y = \frac{Y_{max} \cdot X}{K_D + X}$$

Y = response [RU]

X = analyte concentration [µM]

Y_{max} = maximum binding [RU]

K_D = dissociation constant [µM]

a**b**

Supplementary Figure 22. SPR sensorgrams displaying the binding response of (a) linear peptide **5a** and (b) stapled peptide **5b** to streptavidin immobilised on a CM5 chip in single kinetics mode. Rounded concentrations (in μ M) are shown above the respective response peaks.

Protease inhibition assay

This protocol was adapted from previous research.^{4,5} The Zika virus protease NS2B-NS3 activity assay was carried out in black polypropylene 96-well plates (Greiner Bio-One, Austria) and monitored using an Infinite 200 PRO M Plex microplate reader (Tecan, Switzerland). Experiments were performed in triplicate in aqueous buffer (10 mM Tris-HCl pH 8.5, 1 mM CHAPS, 20% v/v glycerol) using 100 μ L reaction volumes. Linear (**6a**) and stapled (**6b**) peptides were exposed to NS2B-NS3 at different concentrations, with a final enzyme concentration of 0.5 nM. The subsequent addition of NS2B-NS3 substrate (Bz-Nle-Lys-Lys-Arg-AMC) to 5 μ M (additionally 1.5, 12.5, and 20 μ M for **6b**) initiated the enzymatic reaction, whereby the release of AMC was observed for 3 min at 460 nm using an excitation wavelength of 360 nm. Initial velocities of cleavage reaction controls were obtained from the change of fluorescence over time. Inhibition percentages were calculated from the change in initial velocity compared to control reactions without inhibitor present, which were considered as 100% enzymatic activity. The data were analysed and visualised in GraphPad Prism 10 (Dotmatics, USA). For the analysis of dose-response curves, the sigmoidal four-parameter logistic curve model (**Supplementary Equation 3**) was chosen. For the determination of K_i values, the competitive inhibition model (**Supplementary Equation 4**) was chosen due to the presence of the Zika protease recognition motif in peptides **6a** and **6b**.

Supplementary Equation 3.

$$Y = B + \frac{T - B}{10^{H \cdot (\log IC_{50} - X)} + 1}$$

Y = inhibition [%]

B = bottom [%]; constrained to 0

T = top [%]; constrained to 100

H = hill slope [unitless]; constrained to 1

$\log IC_{50}$ = logarithm of half-maximal inhibition concentration [log units]

X = logarithm of inhibitor concentration [log units]

Supplementary Equation 4.

$$Y = \frac{V_{max} \cdot X}{K_m \cdot \left(\frac{I}{K_I} + 1\right) + X}$$

Y = enzyme activity [RFU/s]

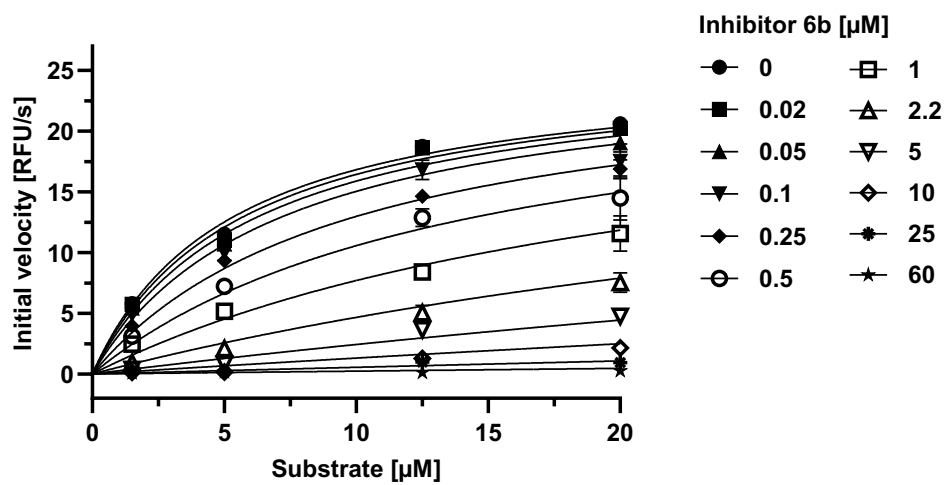
V_{max} = maximum enzyme velocity [RFU/s]

X = substrate concentration [μ M]

K_m = Michaelis-Menten constant [μ M]

I = inhibitor concentration [μ M]

K_I = inhibition constant [μ M]



Supplementary Figure 23. Michaelis-Menten kinetics of the Zika virus protease at different concentrations of inhibitor **6b** ($K_i = 291$ nM).

Protease stability assay

This protocol was inspired by previous experiments by Nitsche et al. and Luo and co-workers.^{4, 6} Peptides (**6a**, **6b**) were exposed to 0.01 eq Zika virus protease (10 μM) in aqueous buffer (10 mM Tris-HCl pH 8.5) in 200 μL reaction volume at 1 mM and kept on a shaking incubator at 37 $^{\circ}\text{C}$. Aliquots of the reaction were taken and quenched by the addition of trifluoroacetic acid to 0.25% v/v and monitored by LCMS using method I at various timepoints until full digestion (10, 20, 30, 45, 60, 90, 120, 150, 180, 240, 300 min). A control of the peptides in the reaction buffer containing 0.25% v/v TFA without Zika virus protease served as reference before the enzymatic digest. The percent abundance of remaining non-enzymatically hydrolysed peptide was determined by peak integration at 254 nm. The data were plotted in GraphPad Prism (Dotmatics, USA), whereby the digest was analysed using the one-phase decay model (**Supplementary Equation 5**).

Supplementary Equation 5.

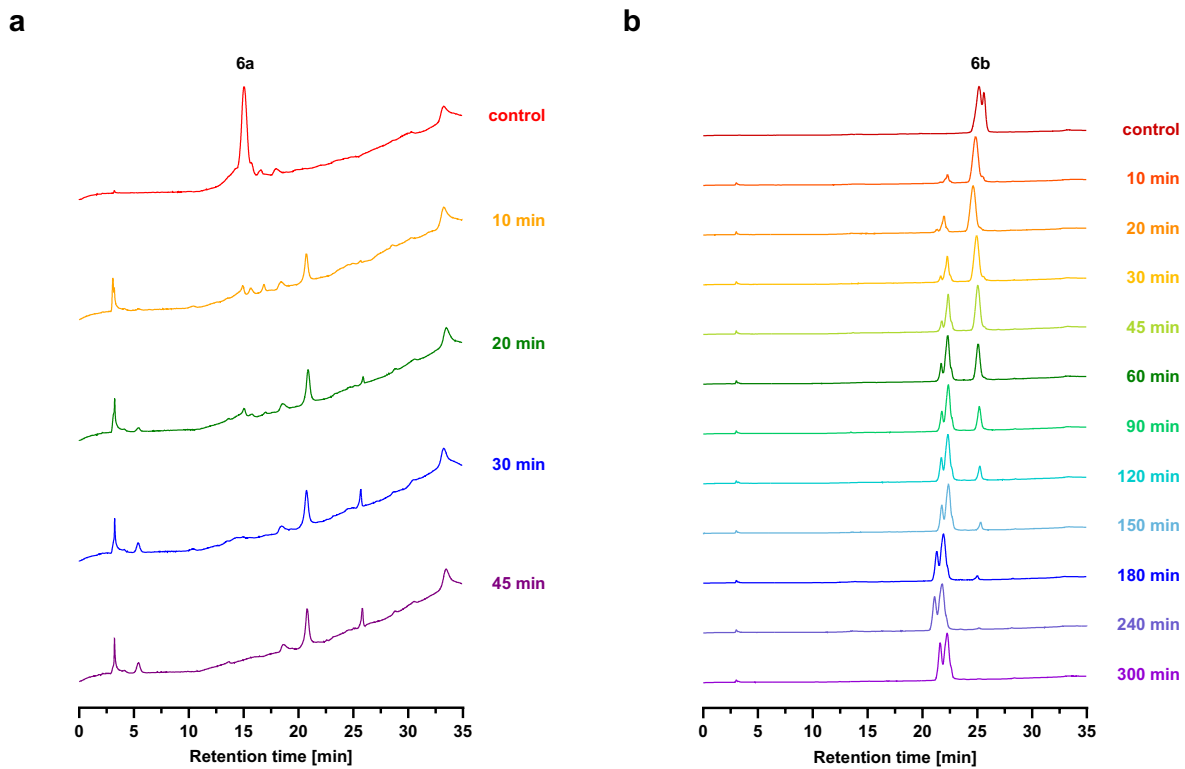
$$Y = (Y_0 - P) \cdot e^{(-K \cdot X)} + P$$

Y = remaining peptide [%]

X = times [min]

Y_0 = peptide abundance at time 0 [%]; constrained to 100

P = plateau; constrained to 0



Supplementary Figure 24. LCMS traces (254 nm) of Zika protease digest (method I) of (a) **6a** and (b) **6b**. Control peak of **6b** appears with shoulder due to hydrolysis of the thiazoline⁵ due to TFA addition.

Protein expression

A pET-29b(+) vector encoding for the respective His-tagged protein of interest between NdeI and XhoI restriction sites was obtained commercially (Twist Bioscience, USA) and transformed into electrocompetent *Escherichia coli* BL21 (DE3) cells (New England Biolabs, USA) using a MicroPulser Electroporator (Bio-Rad, USA). After electrotransfer, the cells were kept at 37 °C for 40 min in SOC medium before plating them on kanamycin-containing (50 µg/mL) LB agar plates for overnight incubation at 37 °C. Three colonies were taken into 10 mL kanamycin-containing LB medium and grown overnight at 37 °C in a shaking incubator. The starter culture was transferred into a culture flask containing 1 L of kanamycin-containing LB medium and grown in a shaking incubator at 37 °C until an OD₆₀₀ of 0.6–0.8 was reached. The culture was allowed to reach room temperature before IPTG was added to a concentration of 1 mM to induce recombinant protein expression. The culture was then kept overnight in a shaking incubator at 18 °C (for Zika virus protease and MBP-TEV protease expression) or at room temperature (for GFP-CX₇C-pIII fusion protein expression).

Protein purification

After expression, the cells were pelleted with a refrigerated high-speed centrifuge (Hitachi, Japan) at $3000 \times g$ for 20 min at 4 °C and resuspended in binding buffer (50 mM Tris-HCl pH 7.5, 300 mM NaCl, 5 mM imidazole, 10% v/v glycerol). The cells were kept on ice during lysis with a high-powered ultrasonic homogeniser (Omni International, USA) for 2×5 min at 60% power and 50% pulse. The supernatant resulting from centrifugation at $16500 \times g$ for 1 h at 4 °C was loaded on a 5 mL HisTrap HP column (Cytiva, USA) for FPLC purification using an ÄKTA pure 25 system (Cytiva, USA). Elution buffer (50 mM Tris-HCl pH 7.5, 300 mM NaCl, 300 mM imidazole, 10% v/v glycerol) was used to remove the His-tagged protein from the Ni-NTA column. After elution, a HiPrep Desalting 26/10 column (Cytiva, USA) was used to transfer the purified protein into desalting buffer (50 mM Tris-HCl pH 7.5, 300 mM NaCl, 1 mM TCEP).

Amicon ultrafiltration devices (Millipore, USA) with a 10 kDa molecular weight cut-off were used for protein concentration. Protein concentrations were measured using a NanoDrop OneC spectrophotometer (Thermo Fisher Scientific, USA) at an absorbance wavelength of 280 nm and extinction coefficients calculated using ExPASy ProtParam (SIB, Switzerland). For long-term storage, proteins were snap-frozen in liquid nitrogen and kept at -80°C .

Both TEV protease and CX₇C-pIII (**9b**) were attached to a fusion partner by an internal TEV protease cleavage site (ENLYFQ↓A/C). Due to autocleavage, no additional release of TEV protease was required. CX₇C-pIII (**9b**) was cut from the original GFP fusion (**9a**) by incubation with 0.1 eq TEV protease overnight at 4 °C in cleavage buffer (50 mM Tris-HCl pH 8.0, 150 mM NaCl, 0.5 mM EDTA, 1 mM TCEP) and subsequent purification by FPLC as previously described. Instead of the elution, the flow-through and wash were combined and buffer-exchanged using an Amicon filter (Millipore, USA) with a 10 kDa molecular weight cut-off.

Protein mass spectrometry

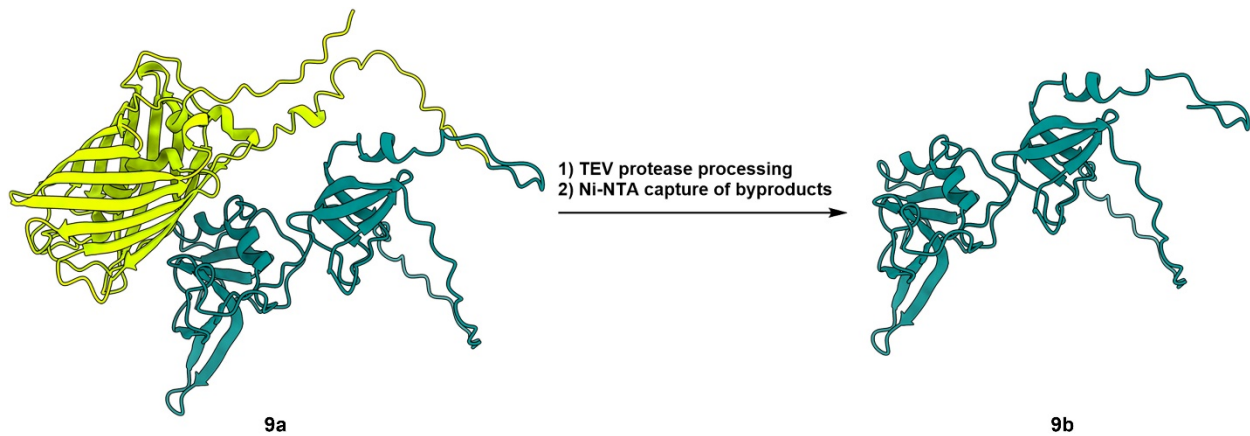
Proteins were analysed using intact protein mass spectrometry performed on an Orbitrap Elite mass spectrometer (Thermo Fisher Scientific) coupled with an UltiMate S4 3000 UHPLC (Thermo Fisher Scientific, USA) using an Agilent ZORBAX SB-C3 Rapid Resolution HT Column (Agilent, USA). Deconvolution was performed using Excalibur 3 (Thermo Fisher Scientific, USA). Expected protein masses were calculated with enviPat Web² (Eawag, Switzerland). Data were plotted and analysed in GraphPad Prism 10 (Dotmatics, USA).

Protein stapling

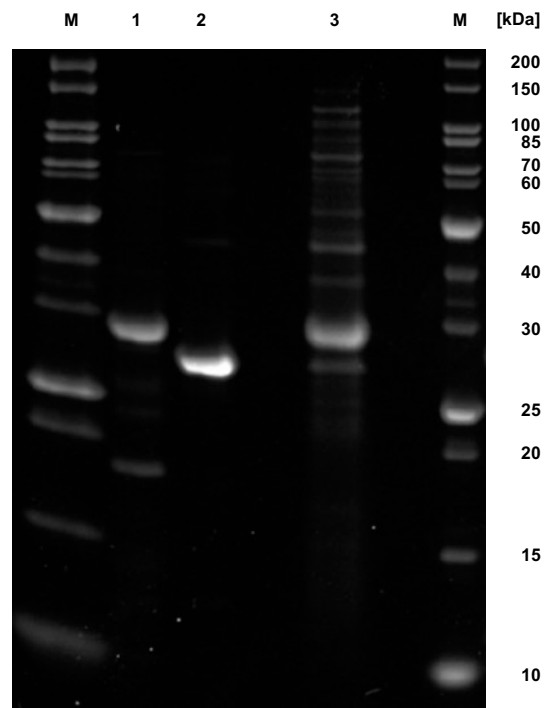
Purified CX₇C-pIII protein (**9b**) was kept in aqueous reducing buffer (50 mM Tris-HCl pH 7.4, 300 mM NaCl, 3 mM TCEP) before exposure to 10 eq of stapling reagent (2-chloromethyl-6-cyanopyridine, **10**; Ambeed, USA) at 150 μM at room temperature for 20 h to give the stapled protein product. The resulting reaction mixture was analysed using intact protein mass spectrometry.

Molecule visualisation

To visualise the resulting protein bioconjugate, the protein fold of 2C-pIII was predicted using ColabFold⁷ and imported to Chimera (UCSF, USA). The N-terminal residues of the resulting model of 2C-pIII (CGSGAGSGC) were removed and the respective stapling product of this peptide with 2-chloromethyl-6-cyanopyridine (**10**) was drawn in ChemDraw (Revvity, USA) and imported into Chimera (UCSF, USA) from its SMILES code using the internal 'Build Structure' function. The stapled peptide was energy-minimised using the internal 'Minimize Structure' function in Chimera (UCSF, USA) before re-attaching it to the remaining protein, after which the whole conjugate was energy-minimised once more. The protein structure was visualised in Chimera X (UCSF, USA). Similarly, the chemical structures shown in the graphical abstract were visualised using Chimera X (UCSF, USA) after importing them from their respective SMILES string.



Supplementary Figure 25. Generation of CX₇C-pIII (**9b**) from GFP-CX₇C-pIII fusion (**9a**).



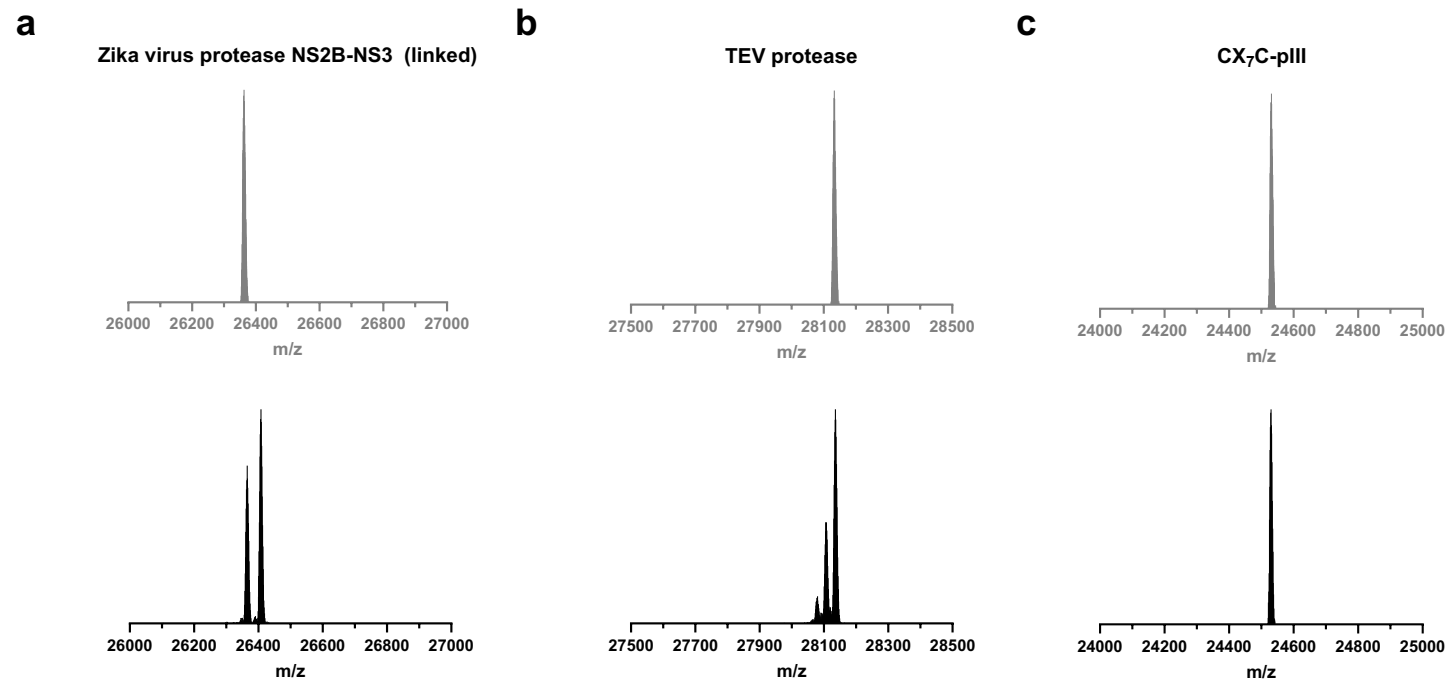
Supplementary Figure 26. Coomassie-stained SDS-PAGE of purified proteins. 1 = Zika virus protease NS2B-NS3 (linked), 2 = TEV protease, 3 = CX₇C-pIII, M = molecular weight marker.

Supplementary Table 3. Amino acid sequences of proteins expressed in this study.

Name	Sequence^[a]	Expression yield in 1 L	Calculated mass^[b]	Observed mass^[b]
Zika virus protease	MMSGKSVDMYIERAGDITWEKDAEVTGNSPRLDVALDESGDFSLVED	59 mg	26363.0	26365.1 ^[c]
NS2B-NS3 (linked)	DGPPMREGGGGSGGGGSGALWDVPAPKEVKKGETTDGVYRVMTRRL GSTQVGVMQEGVFHTMWHVTKGSALRSGEGRLLDPYWGDKQDLVS YCGPWKLDAAWDGHSEVQLLAVPPGERARNIQTLPGIFKTKDGDIGA VALDYPAGTSGSPILDKCGRVIGLYNGVVIKNGSYVSAITQGRREE ETPVEHHHHHH			
MBP-TEV protease	MVIWINGDKGYNGLAEVGKKFEKDTGIKVTVEHPDKLEEKFPQVAAT GDGPDIIFWAHDRFGGYAQSGLLAEITPDKAFQDKLYPFTWDAVRYN GKLIAYPIAVEALSLIYNKDLLPNPPKTWEEIPALDKELKAKGKSAL MFNLQEPYFTWPLIAADGGYAFKYENKDYDIKDVGVNAGAKAGLTF LVDLIKNKHMNADTDYSIAEAAFNKGETAMTINGPWAWSNIDTSKVN YGVTVLPTFKGQPSKPFVGVLSAGINAASPNKELAKEFLENYLLTDE GLEAVNKDKPLGAVALKSYEEELAKDPRIAATMENAQKGEIMPNIPO MSAFWYAVRTAVINAASGRQTVDEALKDAQTLINGDGAGLEVLVFGP ENLYFQAIHHHHHHHGESLFKGPDPYPISSICHILTNESDGHTTS LYGIGFGPFIIITNKHLFRRNNGTLLVQSLHGVFKVKDTTTTLQQHLVD GRDMIIRMPKDFPPFPQKLFREPQREERICLVTTNFQTKSMSSMV SDTSCTFPSSDGI FWKHWIQTKDGQCGSPLVSTRDGFIVGIHSASNF TNTNNYFTSVPKNFMELLTNQEAQQWVSGWRLNADSVLWGGHKVFMV KPEEPFQPVKEATQLMNE	65 mg ^[d]	28133.0	28136.0

GFP-CX ₇ C-pIII	<p>MGSSHHHHHMSKGEELFTGVVPILVELDGDVNGHKFSVRGEGEGDA</p> <p>TNGKITLKLISTTGKLPVPWPTLVTTLGYGVMFARYPDHMKRHDF</p> <p>KSAMPEGYVQERTISFKDDGTFKTRAEVKFEGDTIVNRIKLGIDFK</p> <p>EDGNILGHKLEYNFNHSHKVYITADKQKNGIKANFKIRHNVEDGQSVQL</p> <p>ADHYQQNTPIGDGPVRLPDNHYLSTQSVILEDPNEKRDHMLHEFVT</p> <p>AAGITHGMDELYKGSAGSAAGSGEFENLYFQCGSGAGSGCGGSAET</p> <p>VESCLAKSHTENSFTNVWKDDKTLDRYANYEGCLWNATGVVVCTGDE</p> <p>TQCYGTWVPIGLAIPENEGGGSEGGGSEGGGSEGGGSKPPEYGDTP</p> <p>PGYTYINPLDGTYPGTEQNPANPNPSLEESQPLNTFMFQNNRFRNR</p> <p>QGALTVYTGTVTQGTDPVKTYQYTPVSSKAMYDAYWNGKFRDCAFH</p> <p>SGFNEDLFVCEYQGQSSDLPQPPVNA</p>	24 mg ^[e]	24531.1	24530.1
----------------------------	--	----------------------	---------	---------

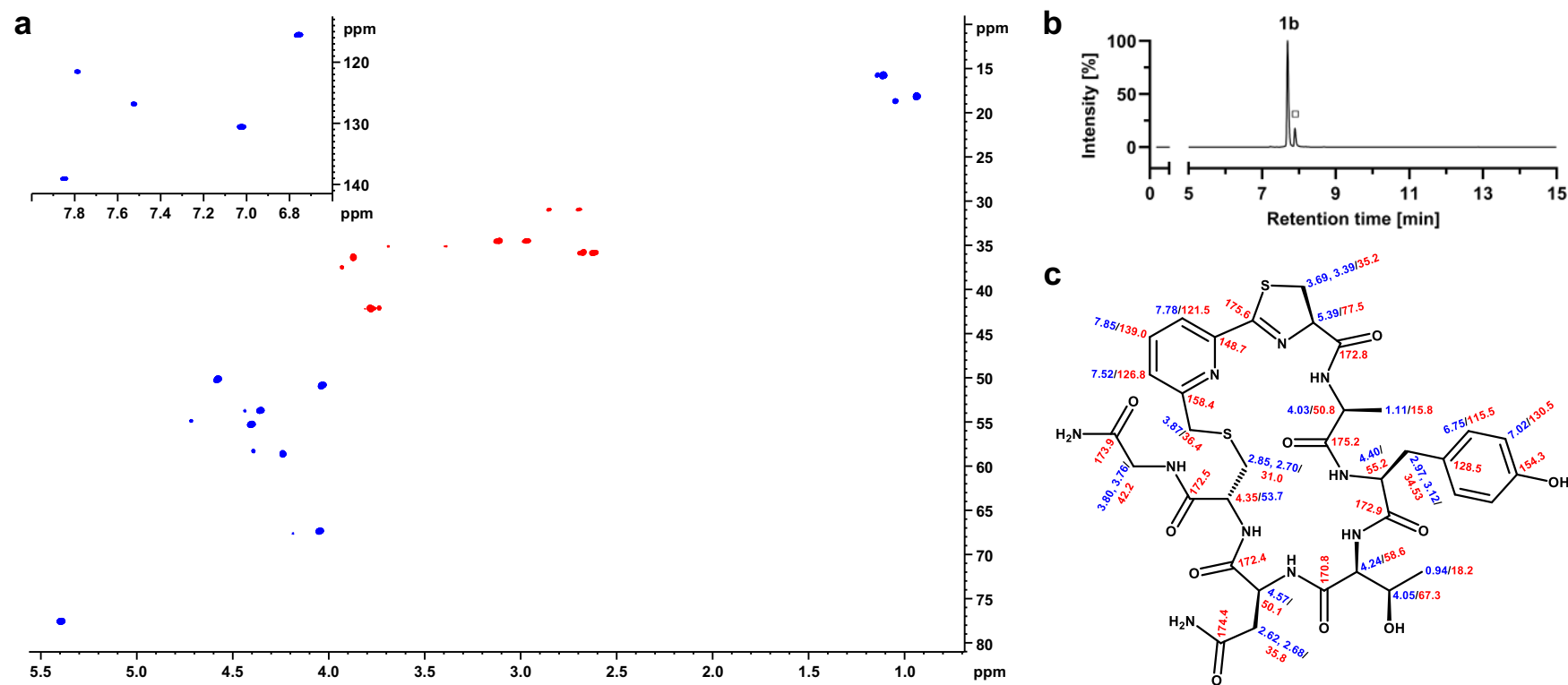
[a] Sequence segment shown in grey was separated by TEV protease cleavage. [b] Calculated and observed masses for the sequence part shown in grey. [c] An acylated species (+42 Da) was also observed for Zika virus protease NS2B-NS3. [d] Yield relative to the sequence segment shown in black. [e] Yield relative to the full sequence.



Supplementary Figure 27. Simulated isotope pattern (grey, top) and intact protein mass spectrum (black, bottom) of (a) Zika virus protease NS2B-NS3 (linked), (b) TEV protease and (c) CX₇C-pIII (**9b**).

NMR spectroscopy

Spectra were recorded on an Ascend 800 MHz NMR spectrometer (Bruker, USA). 2D experiments were recorded to assist the assignment of ^1H and ^{13}C resonances. Chemical shifts are reported in ppm.



Supplementary Figure 28. NMR spectroscopy of stapled peptide **1b** (a) $[\text{}^1\text{H}, \text{}^{13}\text{C}]$ -HSQC spectrum of **1b** (800 MHz, D_2O). Minor peaks correspond to a hydrolysed species. (b) LC trace (280 nm) of the NMR sample of **1b** (method H). Slight hydrolysis of the thiazoline⁵ (\square) occurred due to prolonged exposure to acidic pH at room temperature. (c) ^1H (blue) and ^{13}C (red) chemical shifts are indicated next to the atoms.

Supporting references

- 1 H. J. Bell and L. R. Malins, *Org. Biomol. Chem.*, 2022, **20**, 6250–6256.
- 2 M. Loos, C. Gerber, F. Corona, J. Hollender and H. Singer, *Anal. Chem.*, 2015, **87**, 5738–5744.
- 3 S. Ullrich, U. Somathilake, M. Shang and C. Nitsche, *Commun. Chem.*, 2024, **7**, 143.
- 4 C. Nitsche, H. Onagi, J.-P. Quek, G. Otting, D. Luo and T. Huber, *Org. Lett.*, 2019, **21**, 4709–4712.
- 5 R. Morewood and C. Nitsche, *Chem. Sci.*, 2021, **12**, 669–674.
- 6 W. W. Phoo, Z. Zhang, M. Wirawan, E. J. C. Chew, A. B. L. Chew, J. Kouretova, T. Steinmetzer and D. Luo, *Antivir. Res.*, 2018, **160**, 17–24.
- 7 M. Mirdita, K. Schütze, Y. Moriwaki, L. Heo, S. Ovchinnikov and M. Steinegger, *Nat. Meth.*, 2022, **19**, 679–682.